Norsk Regnesentral
NORWEGIAN COMPUTING CENTER

Report

Remote sensing of snow with passive microwave radiometers

A review of current algorithms

Report no 1019
Authors Jostein Amlien
Date 19 December 2008
ISBN 978-82-539-0529-7

Norsk Regnesentral

Norsk Regnesentral (Norwegian Computing Center, NR) is a private, independent, non-profit foundation established in 1952. NR carries out contract research and development projects in the areas of information and communication technology and applied statistical modeling. The clients are a broad range of industrial, commercial and public service organizations in the national as well as the international market. Our scientific and technical capabilities are further developed in co-operation with The Research Council of Norway and key customers. The results of our projects may take the form of reports, software, prototypes, and short courses. A proof of the confidence and appreciation our clients have for us is given by the fact that most of our new contracts are signed with previous customers.

Front page image: The DMSP satellite. US Department of Defense.

Norsk Regnesentral
Norwegian Computing Center
Postboks 114, Blindern
NO-0314 Oslo, Norway

Besøksadresse
Office address
Gaustadalléen 23
NO-0373 Oslo, Norway

Telefon · telephone
(+47) 22 85 25 00
Telefaks · telefax
(+47) 22 69 76 60

Internett · internet
www.nr.no
E-post · e-mail
nr@nr.no

Title	**Remote sensing of snow with passive microwave radiometers – A review of current algorithms**
Author	**Jostein Amlien**
Quality assurance	
Date	19 desember 2008
Year	2008
ISBN	978-82-539-0529-7
Publication number	Report No 1019

Abstract

This report considers passive microwave radiometry and its application for satellite remote sensing of snow at a global scale. The microwaves observed from a dry snow pack are emitted from the ground beneath the snow. The bulk effect of the snow cover on the microwaves is that the measured brightness temperature will decrease. This depends on the mass of the snow (snow water equivalent – SWE), but also on the snow grain size and internal layering. Other important factors include the forest type. The microwave sensitivity to the snow is strongly dependent on the microwave frequency. The microwave feature to be related to snow is therefore the difference in brightness temperature between two frequencies. Simple empirical algorithms are valid only for limited areas, and global algorithms should therefore consider most of the factors that influence the satellite observations. Radiative transfer models, which aim at predicting the microwave signal from the snow variables, can be valuable for validating algorithms or they may be part of them. As a basis for global algorithm the HUT model and its corresponding algorithms are suggested.

Keywords	Earth observation, snow monitoring, microwave radiometry
Target group	R&D
Availability	Open
Project number	220358
Research field	Earth observation
Number of pages	52

Executive summary

This report considers microwave radiometry and its application for satellite remote sensing of snow, including the detection of snow and the quantification of snow mass/volum.

Microwaves are electromagnetic (EM) waves located close to the radio domain in the EM spectrum, and behaving like high frequency radio waves. Their wavelengths are typically between 1 m and 1 mm (frequency interval 0.3 GHz to 300 GHz). Microwave *radiometry* refers to the use of microwave radiometers for measuring the EM radiation emitted from a target. Microwave radiometry are often referred to as *passive* microwave radiometry (PMR) because radiometers are *passive* instruments, and they should therefore not be confused with radar instruments that actively illuminate the target. In order to compare measurements between different frequency bands, radiometer data is usually quantified in terms of *brightness temperature*, which should not be interpreted as an expression of the physical temperature of the target, but as a representation of the radiance.

Microwaves are able to penetrate dry snow, but the microwave signal from wet snow is completely dominated by the emission from the liquid water contained in the snow near the surface. This prevents the estimation of most snow variables for wet snow. However, a few special algorithms for the detection of wet snow do exist, and due to their high sensitivity to small amounts of liquid water, microwaves are very useful for the forecast of snow melting. The most important feature of the snow with respect to microwaves, is the snow wetness.

Dry snow will neither, or hardly, emit any microwave radiation by itself, nor absorb any of the radiation emitted from the underlying ground. The radiation from beneath will therefore penetrate the snow pack, but due to scattering and refracting effects from snow grains and internal layer interfaces some of the upwelling radiation will return to the ground. The net result is a reduction in the observed brightness temperature. Increased snow amounts will cause more scattering and thus larger reductions.

The scattering of microwaves in a dry snowpack depends on the microwave frequency and the snow grain size. Low frequencies may penetrate through thick layers of fine-grained snow, while higher frequencies and/or larger grain sizes cause more attenuation. The main characteristics of a pack of dry snow that will influence the microwaves are:
1) the amount of snow (snow water equivalent (SWE), or alternatively snow depth)
2) the snow structure (grain size (SGS) and internal layering)
The main challenge in microwave radiometry of snow is therefore to separate the effects of SWE and SGS.

Microwave radiometry of snow can be considered as consisting of two tasks: detection and quantification. The difference in brightness temperature between two channels is a feature that is related to the snow cover, and very useful for both these tasks. The main idea is that the brightness temperature in one frequency, e.g. 37 GHz, decreases significantly due to the snow cover. A lower frequency, e.g. 18 GHz, where the loss is less significant, is used as a reference. The *spectral difference* is defined as the difference in brightness temperatures between two frequencies.

The methods for the *detection* of snow by means of microwave radiometry are beginning to mature. The snow cover can be identified by applying a threshold to the spectral difference. Typically, snow is identified when the spectral difference between 18 GHz and 37 GHz is above zero. Other spectral or polarization differences may also be included in the detection.

The quantification of the snow cover consists of determining its depth (SD) or the corresponding snow water equivalent (SWE). A wide range of empirical algorithms have been developed, but it has proved difficult to extend their application outside their domain. Even between successive years such algorithms may have to be adjusted. However, some improvements have been obtained by approaches that incorporate selected empirical formulas in decision tree algorithms, or even in mixed pixel synthesis, as in the Canadian algorithm (Derksen *et al.* 2005b). It is noted that these approaches require some prior knowledge, e.g. about the vegetation type.

Variables or factors that are important for the microwave signal from snow include snow water equivalent, snow grain size, internal layering, the underlying ground, and the overlying forest vegetation and atmosphere. For global applications, the variation of these factors is significant, and needs to be taken into account. Various algorithms and models have been addressed in the literature, but none of them considers every factor that might be relevant for the retrieval of SWE from microwave data. The combined effect of many variables can be modelled by radiative transfer models (see Mätzler 2006). These models must be sufficiently comprehensive to consider all relevant snow variables, but also sufficiently simple to be inverted easily. This is currently not possible, and no single approach for global SWE retrieval does yet exist. The most promising approaches exploit ancillary data like weather observations in their algorithms.

The most important of the disturbing factors are variations in snow grain size, and in some cold and dry regions it is actually the grain size that is most important for the microwave signal. In these regions the snow depth can be inferred from estimations of the grain size development, where the grain size history is estimated from microwave imagery (Josberger and Mognard 2002). The physical basis is that the grain size development depends on the snow pack temperature gradient, but the method fails when the development slows down.

A more general approach for managing the grain size is to use radiative transfer models, either semi-empirical methods like the HUT model (Pulliainen *et al.* 1999) and the MEMLS model (Wiesmann and Mätzler 1999), or a theoretical model like DMRT (dense media radiative theory) . Of these, only the HUT model is considered suitable for direct use in retrieval algorithms (Mätzler 2006).

An algorithm for global use should be based on physical principles, preferably a radiative transfer model that is possible to invert. It should not be based on satellite data only, but integrate data from other sources as well. The snow variables should show a likely pattern in time and space, and observation and estimation errors should be handled in a statistically sound way.

The recommendation is therefore to use Pullianen's (2006) algorithm, which is a data assimilation algorithm that uses observations from meteorological stations, prior estimates of snow variables and microwave satellite data. The key parameter is the snow grain size, which is used as a fitting parameter in the HUT model and then spatially interpolated for obtaining initial values for the data assimilation

Contents

1 Introduction 9

2 Principles of microwave radiometry 10

2.1 Microwave radiometry in remote sensing 10

2.2 Physical principles 11

2.3 Snow interaction 14

3 Passive microwave radiometers applied for remote sensing of snow 17

3.1 Instruments 17

3.2 Satellites and missions 22

4 Snow signatures and models 23

4.1 Snow signatures 23

4.2 Radiation models for snow 26

5 Algorithms 29

5.1 Snow cover extent 29

5.2 Snow depth and water equivalent 31

5.3 Discussion 40

6 Current operational and prototype products and services 43

6.1 NSIDC 43

6.2 Others 44

7 Discussion and conclusions 45

References 48

1 Introduction

The vision of the EuroCryoClim initiative is to develop new operational services for long-term systematic climate monitoring of the cryosphere. The system and services proposed will be designed to be integrated into the planned international system of systems for global monitoring (GEOSS) – the part of the system aimed for climate monitoring. Based on scientific and technological results from several past and current projects, it is planned to develop a network-based system building on standards and communication languages identified by GMES and GEO for the global system of systems. The network of processing chains and databases will be hosted by mandated organisations in order to ensure long-term and stable operation. The development of this system will draw on the pool of institutions that has developed the current knowledge and technology base for earth observation of the cryosphere and data processing and management. The ambition is that the new system with its accurate climate products will contribute significantly to the monitoring of the global climate.

The aim of the EuroCryoClim Pilot Project is to prepare the ground for a successful development of an operational monitoring system and services in the main project. The pilot project will identify the user needs, develop the design of the system, develop climate demonstration products and a demonstrator of the system, promote the initiative and establish contacts with key users and other key organisations, and develop a work plan for the main project. The Pilot Project is carried out by a group of Norwegian organisations: Norwegian Computing Center (NR), Norwegian Meteorological Institute (met.no), Norwegian Water Resources and Energy Directorate (NVE) and Norwegian Polar Institute (NPI). The project is funded and managed by the Norwegian Space Centre (NSC) and the European Space Agency (ESA).

The snow cover is an important part of the cryosphere. Earth observation of snow can be undertaken by optical sensors, active microwave instruments like radars, or by passive microwave radiometers. While optical remote sensing in the Arctic regions is hampered by the high frequencies of cloud cover, microwaves have the ability to penetrate the clouds. However, active techniques require much energy and will cover only patches of the earth surface. Therefore passive microwave radiometry is often preferred for regular coverage of large areas. This report addresses microwave radiometry of snow covered surfaces, and the techniques for retrieving information about snow cover extent, snow water equivalent and snow depth.

2 Principles of microwave radiometry

This chapter gives a short overview of microwave radiometry in remote sensing (2.1), explains the physical principles of microwave radiation (2.2), and how the microwaves interact with snow (2.3)

2.1 Microwave radiometry in remote sensing

In his textbook "Introduction to microwave remote sensing" Woodhouse (2006) states "The fundamental reason for using microwaves for remote sensing is that they are different". Microwaves interact with physical matter differently than electromagnetic radiation in other wavelength regions. Therefore microwave remote sensing will complement other remote sensing methods. Microwave interactions (e.g. emission, absorption, refraction or scattering) will depend on other physical features than will interactions with optical radiation.

While optical remote sensing started with the invention of the photographic camera, the foundations of microwave remote sensing lie in the study of electricity and magnetism (Woodhouse 2006). The two remote sensing disciplines developed quite independent by following distinct lines of development. Optical remote sensing operates in general between approximately 10 μm (thermal radiation) and 0.5 μm (visible light), and microwaves from 1mm and longer. The separate development has led to separate concepts and terms between the two disciplines.

Like radiowaves, microwaves are detected by means of antennas. The border between the two wave types has traditionally been defined as 1 GHz (30 cm), microwaves being the shorter ones. Since microwave remote sensing may operate at longer wavelengths than this, this terminology is now considered as ambiguous and a bit arbitrary (Woodhouse 2006). Bernier (1987) defined microwaves as the EM spectrum between 1 mm and 1 m (300 to 0.3 GHz) and recommends frequencies higher than 2-3 GHz for snow applications.

One large difference from optical remote sensing is that microwave remote sensing is much more based on fundamental physical principles, represented by Maxwell's electromagnetic equations (Woodhouse 2006). It should be remarked that the term 'remote sensing' in this context includes astronomical observations. The first space platform carrying a microwave radiometer was Mariner 2, which orbited the planet Venus in 1962, six years before the technique was applied for Earth Observation (Woodhouse 2006).

Microwave remote sensing is either active or passive. Active microwave remote sensing, known as radar or SAR, is based on actively submitting a powerful pulse of microwave radiation and measuring its back-scatter from the target. Microwave radiometry is also known as passive microwave remote sensing or passive microwave radiometry (PMR). It is based on the use of a radiometer for passively measuring the weak microwave radiation that is constantly emitted from the earth, including emission from the atmosphere. This report will ignore active techniques and address microwave radiometry only.

In addition to being independent from solar illumination, microwaves are able to penetrate clouds, i.e. the radiation will not be absorbed by the atmosphere. Microwave remote

sensing is therefore said to be independent of weather. Note, however, that microwave radiometry will detect radiation emitted from the atmosphere. The technique of measuring this atmospheric radiation in a wide range of selected wavelengths is known as atmospheric sounding and is a very useful tool for monitoring the atmospheric system.

In contrast to atmospheric sounding, microwave imaging systems aim at measuring radiation that originates from the ground. Such systems should omit wavelengths with significant contribution from the atmosphere. The main physical characteristics that effect the microwave radiation from the ground are in general surface roughness, temperature, salinity and liquid water content (Woodhouse 2006). The microwave radiation from the snow is effected by its wetness, grain size, depth, and density, which will be described in the following chapters.

In addition to penetrating clouds, microwaves will also to some degree penetrate the ground, given dry conditions. In particular, dry snow will be penetrated by microwaves, depending on frequencies. This means that the measured radiation originates from somewhere within the snow layer or from the soil beneath.

For global snow mapping one should note the darkness period during the polar winter, which hamper observations in the optical region, while microwave radiometry will work independent of illumination.

2.2 Physical principles

Electro-magnetic waves

In modern physics electro-magnetic (EM) radiation is considered both as waves and as particles. The best understanding of microwave radiation is obtained by describing it as a wave phenomenon. The formulation of Maxwell's electro-magnetic theory, which describes the relationship between EM radiation and the electric and magnetic fields, was the turning point for the development of microwave remote sensing (Woodhouse 2006). In general the source of EM waves is accelerating charges, usually electrons. The EM waves propagate through space as self-perpetuating oscillating fields, where the electric and magnetic fields induce each other. In the following the magnetic field is omitted because it is similar to the electric field and because most natural substances will interact with the electric field only. In particular, snow does not interact with the magnetic field (Mätzler 1987).

The propagating electric field of EM radiation is a wave moving with the speed of light c, having a wavelength λ and a frequency ν, which are related by $c = \lambda \nu$. It is described as a harmonic function both in space, z (along its propagation direction), and time, t:

$$\mathrm{E}(z,t) = E_0 \sin(kz - \omega t + \phi_0) = E_0 \sin(\phi)$$

where E_0 is the amplitude, ϕ_0 is the initial phase, $\omega = 2\pi\nu$ is the angular frequency, and $k = 2\pi\lambda$ is the wavenumber. Thus the electric field wave has an amplitude E_0 and a phase $\phi = kz - \omega t + \phi_0$. Alternatively the wave function can be formulated as a complex function:

$$\mathrm{E}(z,t) = E_0(\cos(\phi) + \mathrm{i}\sin(\phi)) = E_0 e^{\mathrm{i}\phi}.$$

Radiometric quantities

The *power* of the electric wave has unit W (Watt) and is given by the mean square value of E, scaled by the impedence: $P = E_0^2 / 2\eta$.

Since remote sensing deals with radiation within an area, we need to consider the *power density*, which is simply power per unit area (W/m^2). This quantity is used for describing down-welling and upwelling radiation, which are also referred to as irradiance and exitance, respectively.

The measurements undertaken by a radiometer (or another remote sensing instrument) will represent radiation in certain directions only. The measured quantity is referred to as the *radiance*, which is power density per unit solid angle (W m^{-2} sr^{-1}).

Since the measurements are undertaken within a limited range of frequencies or wavelengths, it is common to scale the radiance according to this range in order to what we commonly refer to as brightness or intensity (Woodhouse 2006). In microwave radiometry the *spectral radiance* is defined as radiance per unit frequency (W m^{-2} sr^{-1} Hz^{-1}). An alternative definition, often used in the optical range, is radiance per unit wavelength (W m^{-2} sr^{-1} m^{-1}).

The EM waves are transverse ones, i.e. the electric and magnetic fields are perpendicular to the direction of propagation. The *polarisation* describes in what direction the electric wave oscillates. It is common to consider the wave as composed of one vertically polarised and one horizontally polarised wave.

Interference and resolution

Interference refers to the combination of two waves $E(z, t) = E_1(z, t) + E_2(z, t)$. Considering two waves having the same frequency and amplitude, they may interfere constructively or destructively, depending on the phase difference. More generally, if we consider the combination of many waves with the same frequency, but different phase and amplitude, their total interference is determined by the sum of the complex numbers $Ee^{i\phi}$. If they sum to zero we will have destructive interference, and if they all go into the same direction the interference will be constructive.

Considering two passive detectors separated by a distance d, and measuring the signal from a radiating source situated in a direction θ relative to the baseline between the two detectors, the phase difference is given by $\delta\phi = 2\pi d \sin\theta / \lambda$.

If we want to find the direction from the measured phase difference, we cannot simply invert the equation because of the ambiguity caused by the 2π modulation of the phase difference. In order to find the look direction we may add more detectors. If we add up a dense line of detectors between the initial two, we may be able to remove most of the sidelobes and thus being able to find the look angle from the phase difference (Woodhouse 2006). The beam width is given by $\theta = 2\lambda / d$. We see that a narrow field of view is obtained by decreasing the wavelength or increasing the width of the detector line, which is identical to the aperture length. Shorter wavelengths, which are relevant for microwave remote sensing of snow, will thus have a narrower field of view (finer spatial resolution).

Propagation of microwaves

The propagation of EM radiation through a material is characterized by these properties:

1. The *electric conductivity* describes how easy electrons can move within a material. EM waves will not propagate in conducting materials, but may be reflected. Some materials (metals) are very close to perfect conductors in the microwave region. Non-conducting materials are known as *dielectric*, and will let EM waves propagate.

2. The *magnetic permeability* is high for magnetic mediums, but this term can be ignored for earth observation applications, being close to its vacuum (free space) value.

3. The *electric permittivity* ε is a complex number $\varepsilon = \varepsilon' + i\,\varepsilon''$ and is an important parameter for microwave remote sensing. It has a free space (vacuum) reference value, and most materials have higher values. The relative permittivity ε_r, is the permittivity divided by the free space permittivity. It is also known as the *dielectric constant*, although it is not a constant, but a property of the material. Its real part ε' refers to how much electric energy a material can store, and how fast the EM waves propagate, as it is the square of the refraction index.

   The imaginary part ε'' of the electric permittivity represents the loss of energy when EM waves travel through and is attenuated by a dielectric medium. The attenuation acts logarithmically, and the penetration depth is defined as the point where the power is reduced by the factor e. The penetration depth increases with wavelength, and is given by

$$\delta_p = \lambda\sqrt{\varepsilon_r'} \Big/ 2\pi\varepsilon_r''$$

Microwave emission

The source of energy is microwave radiometry is *thermal radiation* from the target, i.e. the earth. Thermal radiation originates from the heat energy in matter, which is the random motion of particles. Since EM radiation is caused by the random movement of charges, the emission is spread over a wide spectral band. Planck's law expresses the relationship between spectral radiance I, absolute temperature T and frequency ν for a *blackbody*, i.e. a body where there is free exchange of energy at its borders.

$$I = \frac{2\mathrm{h}\nu^3/\mathrm{c}^2}{e^{\mathrm{h}\nu/\mathrm{k}T} - 1}$$

For microwaves we approximate $e^{\mathrm{h}\nu/\mathrm{k}T} - 1 = \mathrm{h}\nu/\mathrm{k}T$, and Planck's equation simplifies into

$$I = \frac{2\nu^2\mathrm{k}}{\mathrm{c}^2}T$$

which is known as the Rayleigh-Jeans law. These laws refer to a theoretical blackbody, but in the real world the actual emitted radiance from an object will be reduced by an *emissivity* factor, ε:

$$I = \varepsilon\frac{2\nu^2\mathrm{k}}{\mathrm{c}^2}T$$

The emissivity is in general dependent on the frequency, since physical objects typically are selective radiators. For radiances measured in a specific frequency, ν, we must therefore consider the *spectral emissivity*, ε_ν.

Note that in the literature and in this report the symbol ε is used for the representation of the emissivity as well as the electric permittivity, depending on the context. These two properties are not equivalent, and they should therefore not be intermixed.

According to the Rayleigh-Jeans law, I is proportional to T, so we can easily retrieve a T from a measurement of I. Independent of the actual physical temperature of the target, we refer to this T as the *brightness temperature*, more specifically as the Rayleigh-Jeans brightness temperature.

In microwave radiometry, the radiance is mostly expressed in terms of the brightness temperature, T_B. Note that the brightness temperature is just another way to express the measured radiance and should never be interpreted as any approximation to the real temperature. In order to separate the two, we may refer to the brightness temperature by adding a subscript: T_B. Since T_B is a measured quantity, it will depend on the frequency ν, and we may consequently use T_ν, or e.g. T_{17} when measured in the 17 GHz frequency band.

The relationship between the radiance I_ν and brightness temperature T_ν, which are quantities measured in the frequency ν, and the real physical temperature T, can be expressed as

$$I_\nu = \frac{2\nu^2 \mathrm{k}}{\mathrm{c}^2} T_\nu = \varepsilon_\nu \frac{2\nu^2 \mathrm{k}}{\mathrm{c}^2} T$$

which leads to

$$T = T_\nu / \varepsilon_\nu$$

The reader may now miss the Stephan-Boltzman law or Wien's displacement law, which are important for thermal remote sensing. For microwaves they are not very relevant, though.

Finally we note Kirchoff's radiation law, which states that good absorbers are good emitters. More precisely the spectral emissivity also expresses the spectral absorbance. This implies that high absorption is related to high emission, where low absorption are related to low emission and more reflection, scattering and transmission

2.3 Snow interaction

The propagation of microwaves in a snowpack is characterised by the fact that the snow grains are smaller than or comparable to the wavelength in size. The presence or absence of liquid water have a significant importance.

From a physicist's point of view, the interaction of microwaves with snow is of particular interest or challenge due to the extremely difficult boundary conditions for solving the Maxwell equations (Mätzler 1987). From a non-physicist's point of view, this subject is therefore characterized by a lot of literature that are challenging to understand.

Snow is a mixture of ice, air, and possibly liquid water. The effective dielectric constant for a snow pack will be a weighted average of the dielectric constants for ice and water, while

the influence from the air inside the snow layer can be ignored, since $\varepsilon' = 1$. The dielectric constants for ice and water are extremely different, though. Their dependencies on frequency can both be described as a Debye type relaxation spectrum, which can be derived from the dipole moment of the water molecule (Mätzler 1987). Such a spectrum will have a unimodal distribution where the loss is maximised at a given frequency, referred to as the *relaxation frequency*.

Dry snow

The influence of ice on the microwave spectrum is weak. The real part of the dielectric constant is independent of frequency, with a typical value of $\varepsilon' = 3.2$ (Bernier 1987) or $\varepsilon' = 3.17$ (Mätzler 1987). Its imaginary part (quantifying the loss) is very low in the microwave region ($\varepsilon'' \approx 0$), since the relaxation frequency is located in the kHz range, i.e. in the long-wave radio domain. The loss decreases with increasing frequency up to 1 GHz, where it starts slowly increasing again as an effect of the tails of the infrared absorption bands. For dry snow, consisting of ice grains and air, the real part of the dielectric constant is dependent on the snow density (Künzi *et al.* 1982; Mätzler 1987).

Scattering will occur in any inhomogeneous dielectric medium, like snow. The scattering in a snow pack is caused by dielectric discontinuities between snow grains and air (Bernier 1987). It requires that the wavelengths are comparable to the snow grain size, i.e. in the higher microwave frequencies. Since dry snow will absorb very little of the radiation, the microwaves are allowed to penetrate and scatter over distances that are long compared to the wavelength, which results in volume scattering. Refraction at internal layer interfaces is also important.

When the snow grains are smaller than the microwaves, they will act like quasi-diffuse Rayleigh scatters. The scattering will increase with grain size and with frequency (Mätzler 1987). For the highest frequencies where the wavelengths are smaller than the grain size, the scattering will be strong even at a very thin snow cover, while the lowest frequencies (<2 GHz) hardly will interact with seasonal dry snow at all (Bernier 1987). Between these limits, the microwave scattering will yield information about the snow pack.

Since dry snow has a low emissivity, the main source of microwave radiation must be beneath the snow. Dry or frozen ground are good emitters (Bernier 1987), but when the radiation is scattered, some of it will be scattered back to the ground and be absorbed. In addition, multiple scattering will increase the absorption in the snow pack itself. One important effect of volume scattering in a thick snow pack is therefore a reduction in the brightness temperature (Bernier 1987). Snow on polar ice sheets will have signatures that differ from perennial snow (see Mätzler *et al.* 2006).

Impurities in the ice will enhance the absorption of microwaves. The low absorption for ice makes ice and dry snow sinsitive to additional factors like impurities. (Künzi *et al.* 1982; Mätzler 1987).

Wet snow

The influence of liquid water on the microwave spectrum of snow is huge. The relaxation frequency of liquid water is located in the X-band at 10 GHz, while the real part of the permittivity is strongly decreasing with increasing frequency throughout the microwave

domain. The relaxation frequency for wet snow, which typically contains up to 10% of liquid water, may be higher than for liquid water itself (Mätzler 1987). The relaxation frequency will also depend on the shape of the liquid inclusions and the liquid water content. The absorption in wet snow is several orders of magnitude higher than for dry snow, turning volume scattering completely off (Mätzler 1987).

Although the scattering signature appearing for dry snow will disappear when the snow becomes wet, the polarization difference is almost unchanged (Mätzler and Hüppi 1989; Grody and Basist 1996).

3 Passive microwave radiometers applied for remote sensing of snow

3.1 Instruments

SMMR

The Scanning Multichannel Microwave Radiometer (SMMR) was launched by Nimbus-7 in 1978. SMMR had five frequencies for both vertical and horizontal polarizations, see Tab. 3.1. The cell size of the grid is 25 km (http://nsidc.org/data/nsidc-0071.html). Global coverage data is available for the period between 25 October 1978 and 20 August 1987.

Table 3.1. *SSMR characteristics (Hall 1986; Derksen et al. 2005a)*

Center frequency	6.6 GHz	10.69 GHz	18.6 GHz	21.0 GHz	37.0 GHz
Sensitivity	0.9 K	0.9 K	1.2 K	1.5 K	1.5 K
IFOV \ km	148 x 95	91 x 59	55 x 41	46 x 30	27 x 18
Beam width	4.2°	2.6°	1.6°	1.4°	0.8°

SSM/I

The SMMR was succeeded by the Special Sensor Microwave Imager (SSM/I). It has been flown by the DMSP satellites since 1987, and is currently flown by the DMSP F13 satellite (Tedesco and Miller 2007). It is a 4 frequency, conically scanning microwave radiometer. All frequencies operate in dual polarization, but vertically polarized only at 22 GHz. Tab. 3.2 shows how the characteristics vary with frequency.

The data are grided into 25 / 12.5 km resolution cells. The spatial resolution (IFOV) is defined as the half-power (3 dB) beam-width, which projects as an ellipsoid on the Earth surface. The ellipsoid axes are much larger then the sampling interval for the lower frequencies, see Tab. 3.2.

Table 3.2. *SSM/I characteristics (http://mrain.atmos.colostate.edu/LEVEL1C/level1C_devssmi.html)*

Center frequency	19.35 GHz	22.235 GHz	37.0 GHz	85.5 GHz
Polarization	V / H	V	V / H	V / H
Band width	0.25 GHz	0.25 GHz	1.0 GHz	1.5 GHz
Sensitivity	0.6 K	0.6 K	0.6 K	1.1 K
IFOV \ km	69 x 43	60 x 40	37 x 28	15 x 13
Sampling rate \ km	25 x 25	25 x 25	25 x 25	12.5 x 12.5
Integration time	7.95 ms	7.95 ms	7.95 ms	3.89 ms
Main beam efficiency	96.1 / 96.5 %	95.5 %	91.4 / 94.0 %	93.2 / 91.1 %
Beam width	1.87°	1.65°	1.10°	0.43°

The scan geometry is depicted in Figs. 3.1 and 3.2. One entire scan comprises ±51.2° across the sub-satellite track, which leads to a swath width of 1400 km. Each complete scan consists of 128 uniformly spaced samples at 85.5 GHz, together with 64 uniformly spaced samples at the lower frequencies for every other scan. The IFOV overlap is largest at the scan edges.

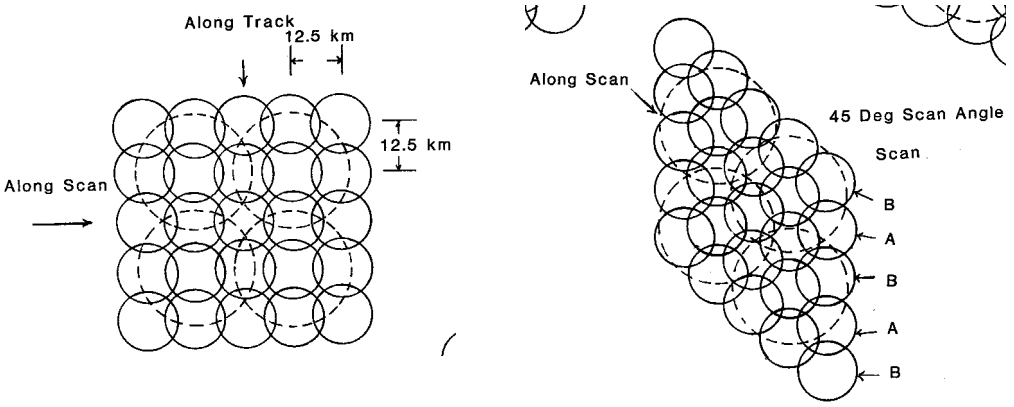

Figure 3.1 Spatial sampling of the SSM/I sensor at 0° (left) and 45° (right) scan angle (Hollinger *et al.* 1987). The circles are the 37 (dashed) and 85 GHz (solid lines) instantaneous field of view (IFOV).

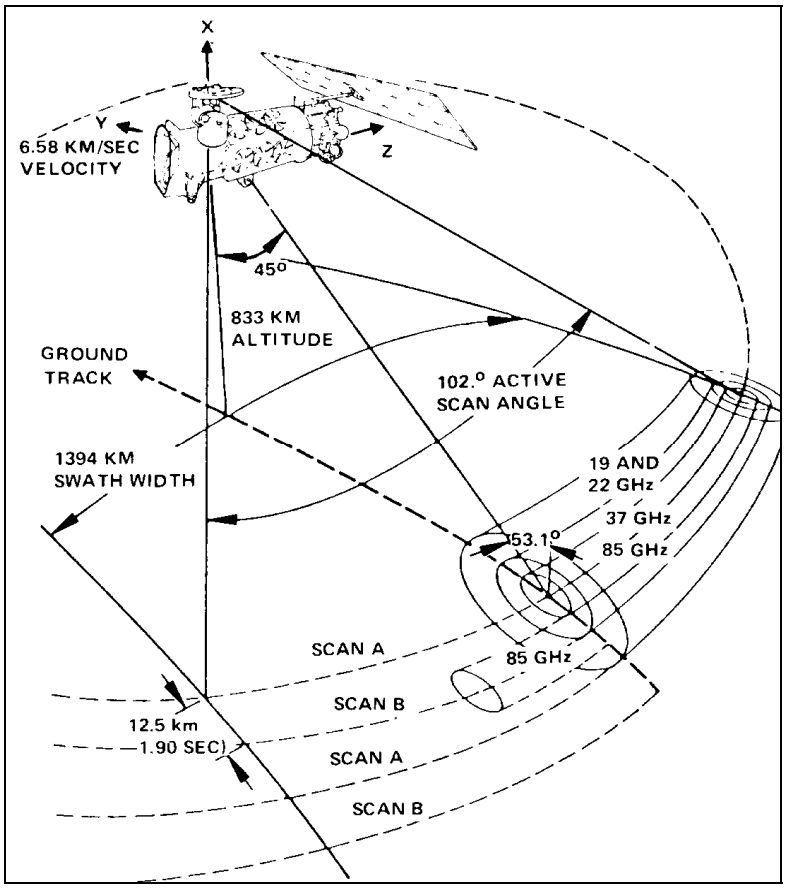

Figure 3.2. Scan geometry of the DMSP-SSM/I system (Hollinger *et al.* 1987). Scan A denotes scans in which all channels are taken, while scan B denotes scans in which only the 85.5 GHz data are measured.

Together the two instruments SMMR and SSSMI/ cover a period of 30 years, but note the difference in frequency characteristics.

SSMIS

The Special Sensor Microwave Imager/Sounder (SSMIS) was launched 18 October 2003 on-board DMSP-F16. It is a combined imager and sounder developed in order to replace the SSM/I, and other operational instruments (SSM/T). SSMIS is a conical scanning radiometer that observes the Earth with a 53.1° incidence angle in 24 channels. The level 1C dataset (http://mrain.atmos.colostate.edu/LEVEL1C/level1C_devssmis.html), consists of eleven channels, and is shown in Tab. 3.3.

The differences from SSM/I include a modification of the 85.5 GHz frequency to 91.7 GHz, additional high frequency channels, and a better brightness temperature sensitivity.

Table 3.3. *Characteristics of SSMIS level 1C subset (http://mrain.atmos.colostate.edu/LEVEL1C/level1C_devssmis.html)*

Center frequency	19.35 GHz	22.235 Hz	37 GHz	91.665 GHz	150 GHz	183.31GHz
Polarization	V / H	V	V / H	V / H	H	H
Band width	0.35 GHz	0.41 GHz	0.16 GHz	1.41 GHz	1.64 GHz	0.51 / 1.02 / 1.53 GHz
Sensitivity	0.35 K	0.45 K	0.22 K	0.19 K	0.53 K	0.38 / 0.39 / 0.56 K
IFOV \ km	73 x 47	73 x 47	41 x 31	14 x 13	14 x 13	14 x 13
Sampling rate \ km	45 x 74	45 x 74	28 x 45	13 x 16	13 x 16	13 x 16

PRIRODA

PRIRODA ("Nature") was the last module of the MIR space station, docked 26 April 1996. It had a wide set of EO instruments (see http://www.ire.rssi.ru/priroda/prir_br.htm). The orbit was near to circular with a height about 360 km over the Earth surface and an inclination of 51.7°. The purpose of Priroda was scientific and experimental. MIR de-orbited 23 March 2001.

The characteristics of the IKAR microwave radiometer system on board Priroda are listed below in Table 3.4. There are three different radiometer systems onboard: a nadir looking radiometer (Ikar-N), a scanning radiometer (Ikar-Delta) and a panoramic radiometer (Ikar-P), working at 40° of the nadir direction.

Table 3.4. *Characteristics of the microwave radiometer system IKAR on board the Priroda module. (http://www.ire.rssi.ru/priroda/Ikar/Ikar.htm)*

Radiometer	Device	Wavelength	Beam width	Sensitivity	Resolution
IKAR-N	R-30	0.3 cm	9°	0.15 K	60 km
IKAR-N	R-80	0.8 cm	9°	0.15 K	60 km
IKAR-N	R-135	1.35 cm	9°	0.15 K	60 km
IKAR-N	R-225	2.25 cm	9°	0.15 K	60 km
IKAR-N	R-600	6.0 cm	9°	0.15 K	60 km
IKAR-delta	R-80	0.8 cm	1.5°	0.5 K	8 km
IKAR-delta	R-135	1.35 cm	2°	0.4 K	15 km
IKAR-delta	R-225	2.25 cm	n/a	n/a	n/a
IKAR-delta	R-400	4.0 cm	5°-7°	0.15 K	50 km
IKAR-P	R-225	2.25 cm	5°-7°	0.15 K	75 km
IKAR-P	R-600	6.0 cm	12°	0.15 K	75 km

AMSR-E

The Advanced Microwave Scanning Radiometer – EOS (AMSR-E) is carried by the EOS Aqua satellite. It operates in dual polarisation in 6 frequencies. Tab. 3.5 shows the spatial resolutions and other characteristics for each frequency.

Table 3.5. *AMSR-E characteristics (http://mrain.atmos.colostate.edu/LEVEL1C/level1C_devamsr.html)*

Center frequency	6.925GHz	10.65GHz	18.7 GHz	23.8 GHz	36.5 GHz	89.0 GHz
Polarization	V / H	V / H	V / H	V / H	V / H	V / H
Band width	0.35 GHz	0.1 GHz	0.2 GHz	0.4 GHz	1.0 GHz	3.0 GHz
Sensitivity	0.3 K	0.6 K	0.6 K	0.6 K	0.6 K	1.1 K
IFOV \ km	74 x 43	51 x 30	27 x 16	31 x 18	14 x 8	6 x 4
Sampling rate \ km	10 x 10	10 x 10	10 x 10	10 x 10	10 x 10	5 x 5
Integration time	2.6 ms	2.6 ms	2.6 ms	2.6 ms	2.6 ms	1.3 ms
Main beam effic.	95.3%	95.0%	96.4%	96.4%	95.3%	96.0%
Beam width	2.2°	1.4°	0.8°	0.9°	0.4°	0.18°

Note that the sampling rate is denser than the IFOV. The instrument rotates around its vertical axis every 1.5 second, and views the Earth from an altitude of 705 km with a fixed incidence angle of 53.9°. Each scan is a 70° arc on the Earth surface about the sub-satellite track, and the swath is 1500 km wide.

The following detailed description of AMSR-E is given by Solberg *et al.* (1997 ch. 7.2):

> "The instrument consists of an offset parabolic reflector 1.6 meters in diameter, fed by an array of six feedhorns. The reflector and feedhorn arrays are mounted on a drum, which contains the radiometers, digital data subsystem, mechanical scanning subsystem, and power subsystem. The reflector/feed/drum assembly is rotated about the axis of the drum by a coaxially mounted bearing and power transfer assembly. All data, commands, timing and telemetry signals, and power pass through the assembly on slip ring connectors to the rotating assembly.
>
> A cold load reflector and a warm load are mounted on the transfer assembly shaft and do not rotate with the drum assembly. They are positioned off axis such that they pass between the feedhorn array and the parabolic reflector, occulting it once each scan. The cold load reflector reflects cold sky radiation into the feedhorn array, thus serving, along with the warm load, as calibration references for the AMSR. Calibration of the radiometers is essential for collection of useful data. Corrections for spillover and antenna pattern effects are incorporated in the data processing algorithms.
>
> The AMSR rotates continuously about an axis parallel to the local spacecraft vertical at 40 rpm. At an altitude of 705 km, it measures the upwelling scene brightness temperatures over an angular sector of ±61 degrees about the sub-satellite track, resulting in a swath width of 1445 km. During a period of 1.5 seconds, the spacecraft sub-satellite point travels 10 km. Even though the instantaneous field-of-view for each channel is different, active scene measurements are recorded at equal intervals of 10 km (5 km for the 89 GHz channels) along the scan. The half cone angle at which the reflector is fixed is 47.4 degrees, which results in an Earth incidence angle of 55.0 degrees."

AMSR-E is a modification of the AMSR on the Japanese Advanced Earth Observing Satellite-II (ADEOS-II). AMSR has two additional, vertically polarized channels at 50.3 and 52.8 GHz. AMRS2 is a modified version of AMRS that will be mounted onboard JAXA's GCOM satellite.

Overview

An overview of the presented instrument is given in Table 3.6.

Table 3.6. *Overview over microwave satellite instruments.*

Instrument	Mission	Availability	Cell size	Comments
SMMR	Nimbus	25 Oct 1978 – 20 Aug 1987	25 km	
SSM/I	DMSP	July 1987 – present	12.5 –25 km	
SSMIS	DMSP	18 Oct 2003 – present	13 – 74 km	Replaces SSM/I
AMSR	ADEOS-II	2003 – present	5 – 50 km	
AMSR-E	EOS Aqua	4 May 2002 – present	5 – 10 km	Modifid from AMSR
AMSR2	GCOM-W	planned		Future JAXA mission
PRIRODA	MIR	26 Apr 1996 – 23 Mar 2001	8 – 65 km	

3.2 Satellites and missions

DMSP

The Defence Meteorological Satellite Program (DMSP) satellites carry a wide range of operational instruments. The SSM/I has been carried by these satellites since DMSP F-8. The Special Sensor Microwave Imager Sounder (SSMIS) replaced SSM/I from F-16.

Each DMSP satellite follows a near circular, sun synchronous, and near polar orbit. The main DMSP orbital characteristics are presented in Table 3.7. The orbit provides complete coverage of the Earth, except for two small circular sectors 2.4° centred on the North and South poles.

Table 3.7*. Main orbital characteristics of the DMSP satellites. Compiled from NASA (http://nssdc.gsfc.nasa.gov/nmc/SpacecraftQuery.jsp).*

Plat-form	Instrument	Altitude [km]	Inclination	Period [min]	Eccentricity	Launch date	Date of last data
F8	SSM/I	564-653	97.6	96.9	0.0064	20 Jun 1987	1 Aug 1994
F9	SSM/I	819	98.6°	101.2	0	3 Feb 1988	3 Apr 1992
F10	SSM/I	564-653	97.6°	96.9	0.0078	1 Dec 1990	26 Sep 1994
F11	SSM/I	846-870	98.9°	101.9	0.00166	28 Nov 1991	16 May 2000
F12	SSM/I	839-856	98.9°	101.9	0.00118	29 Aug 1994	operating
F13	SSM/I	845-851	98.8°	101.9	0.00041	24 Mar 1995	operating
F14	SSM/I	843-854	98.9°	101.8	0.00076	4 April 1997	operating
F15	SSM/I	837-851	98.9°	101.8	0.00097	12 Dec 1999	operating
F16	SSMIS	843-853	98.9°	101.9	0.00069	18 Oct 2003	operating
F17	SSMIS	841-855	98.9°	102.0	0.00097	4 Nov 2006	operating

EOS Aqua

EOS Aqua was launched 4 May 2002 by NASA. It is the second major component of the Earth Observing System (EOS) following Terra (launched 1999) and followed by Aura (launched 2004). The aim of Aqua (EOS PM-1) is to study precipitation, evaporation and the water cycle. In addition to AMRS-E it carries one MODIS instrument and four instruments for studying the atmosphere.

GCOM-W

The Global Change Observation Mission (GCOM) is being planned by JAXA as a follow-up to ADEOS. GCOM-W is primarily a sea surface mission. It will carry the AMSR2 instrument. GCOM is JAXA's contribution to the GEOSS initiative (http://directory.eoportal.org/presentations/330/14848.html).

4 Snow signatures and models

In order to be able to retrieve information about snow variables, like depth, water equivalent, density, structure and wetness from microwave measurements, it is necessary to know how these variables are related to the microwave brightness temperatures for different instrument settings, i.e. frequency, polarization, and view angle.

Such relationships can be expressed in terms of empirical snow signatures, where a given snow variable is linked more or less directly to a measureable EM quantity. One can also establish physically based models that predict the EM quantities from a set of snow variables. In practice the distinction between these two approaches in not always strict and clear.

4.1 Snow signatures

Microwave signatures for snow have been established through ground-based studies during decades. 30 years ago Hofer and Schanda (1978) reported the first results of a high-altitude Alpine test site, and they concluded that microwave radiometry is very sensitive to the snow wetness, and that volume scattering is important in dry snow packages. Later studies have confirmed that the microwave signatures for seasonal snow show a large contrast between wet and dry snow, that the brightness temperature for dry snow decreases with frequency, and that volumes of dry snow may potentially be estimated (Mätzler *et al.* 2006). Stiles and Ulaby (1980) found that the emissivity of wet snow increased with snow wetness, with higher sensitivity at higher frequencies.

Dry snow

When moving from snow-free to dry snow-covered surfaces, the brightness temperature will show a sharp decrease. This decrease is a unique feature for snow and can therefore be used as reliable indicator of dry snow (Mätzler 1994).

Field observations made by Ulaby and Stiles (1980) showed that the brightness temperature, T_B, depends on the snowpack water equivalent, but also on frequency and incidence angle. The inverse relationship between T_B and SWE was also reported by Halllikanen (1989) for dry snow. When the amount of dry snow increases, the upwelling radiance will decrease due to the increased scattering, and the obtained brightness temperature will consequently decrease. The inverse relationship between SWE and brightness temperature has been observed by several authors (see Bernier 1987). This effect is best observed at higher frequencies. Macelloni *et al.* (2001) compared experimental and model results, and found T_{37V} to be sensitive to SWE, but hardly T_{10V}.

The decreasing brightness temperature with increasing frequency is a unique feature for dry snow on land and is therefore the most useful snow signature (Mätzler 1987). This signature is the basis the spectral gradient method (Künzi *et al.* 1982), which requires data from a multi-frequency instrument. The spectral gradient between two spectral channels is defined as their difference in brightness temperature divided by their frequency difference. The similar term *spectral difference* refers simply to the brightness temperature difference.

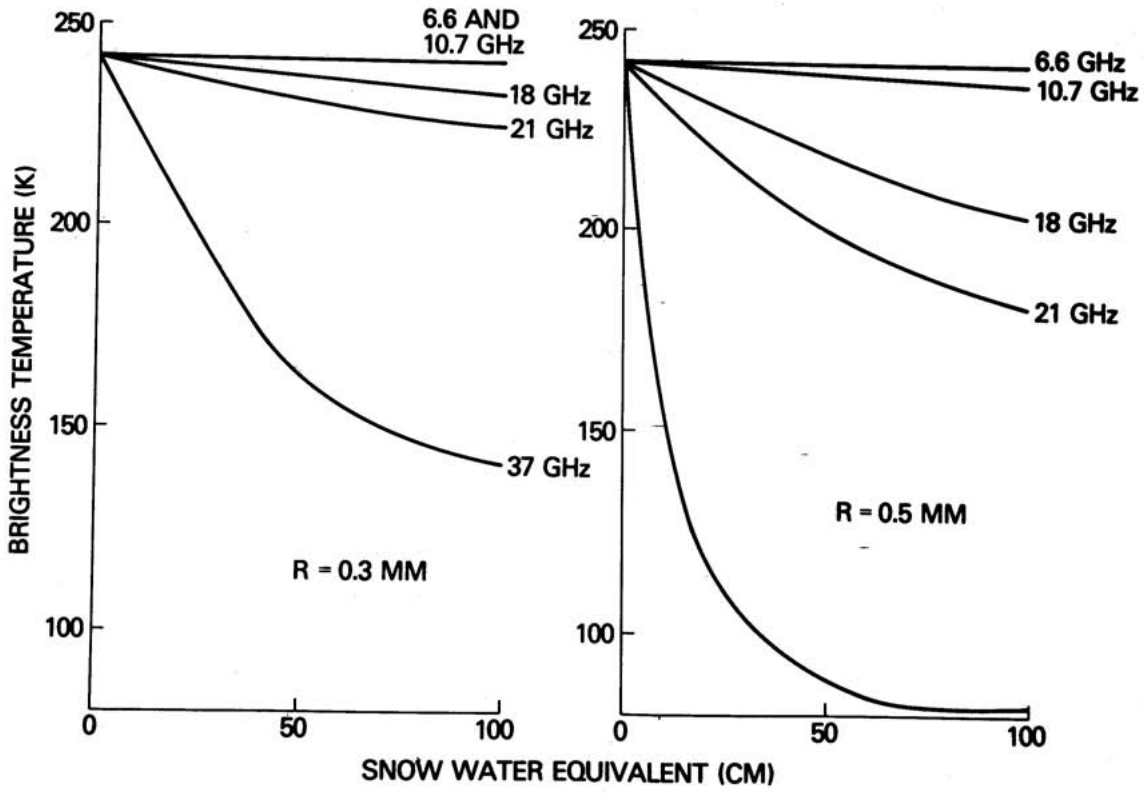

Figure 4.1. Computed brightness temperature vs. SWE for SMMR frequencies (Chang 1986). Note the significant importance of the grain size (left: 0.3 mm; right: 0.5 mm)

Mie theories for scattering have been applied for calculating microwave signatures for snow (Chang 1986). Fig. 4.1 shows brightness temperatures vs. SWE for various grain sizes and frequencies. We see that the brightness temperature of snow will decrease with frequency, and with SWE and grain size.

The spectral gradient is suitable for separating snow from other land surfaces and for the estimation of SWE (Mätzler 1994). The spectral gradient is more sensitive in higher frequencies (Grody and Basist 1996), but experiments (Tait *et al.* 1999) in the millimetre range have demonstrated that the spectral gradient will be influenced by atmospheric attenuation.

The dry snow spectral gradient is present in both polarizations. The gradient in vertical polarization is more sensitive to variations in SWE than is horizontal polarization. It will therefore be able to detect a more shallow snow-cover (Grody and Basist 1996). However, in global applications confusion with dry desert soils might be a problem. The problem can be reduced by using horizontally polarized data for the spectral gradient.

Hallikainen (1989) considered the temporal change in the spectral gradient from snow-free conditions, and found that these changes could be related to SWE.

Mätzler (1994) examined spectral emissivity signatures for many relevant surface types in order to examine how snow separates from non-snow in areas with different surface signa-

tures. An ideal on-off situation for detection of dry snow is possible for frequencies higher than 20 GHz.

The structure of the snow is also related to the brightness temperature. The scattering will increase with increasing grain size and layering (Bernier 1987), but the effect on the brightness temperature may be difficult to interpret.

Vegetation overlying the snow will to a large extent both emit and scatter the radiation and therefore introduce significant variations to the measurements. These effects should therefore be corrected. Tiuri (1982) detected snow cover in forested areas by examining the spectral gradient.

Wet snow

When it comes to wet snow, the characteristic scattering signature from the snow pack is lost due to the absorption and emission from the liquid water. The detection of wet snow must therefore rely on the specific polarisation signature of wet snow (Mätzler 1994).

Liquid water will absorb and re-emit microwaves and consequently reduce both the scattering and the penetration drastically. The observable effect on microwaves is an increased brightness temperature when small amount of liquid water (1 %) is introduced, but larger amounts of liquid water (>15%) will in general not introduce any further increase (Mätzler 1994). Such small amounts are difficult to measure in field, making it very difficult to establish any accurate quantification of the liquid water content (see Bernier 1987). The effect is less at lower frequencies (Stiles and Ulaby 1980). The onset of snow melt is easily detected since the sharp increase in brightness temperature will occur immediately after the release of liquid water (Künzi *et al.* 1982).

Liquid water may a huge problem when separating snow and non-snow areas. Wet soil and dry snow will both appear as cold, while frozen or dry soil and wet snow will both appear as warm (Mätzler *et al.* 1982).

Table 4.1. *Overview of how the microwave measurements are influenced by the main snow characteristics and by instrument settings*

Snow type	Main characteristics	Influence of increasing SWE / SD	Influence of increasing grain size	Effect of microwave frequency	Effect of microwave polarization
Dry snow	Scatters the emission from the ground below	Increases the scattering	Increases the scattering	More scattering at higher frequencies	Minor
Wet snow	Acts like a black body, by absorbing the radiation emitted from the ground and emitting its own radiation	No effect	No effect	More sensitive at higher frequencies	Major (dual polarization needed, but detection still difficult)

4.2 Radiation models for snow

Microwave radiation models for snow aims at predicting the microwave radiation from a snowpack. Such models include many parameters describing snow variables (e.g. grain size, density, thickness, wetness, and layering structure) and EM quantities (e.g. frequency, polarization, incidence angle). A lot of scientific works with microwave remote sensing of snow involve models of some kind. Radiation models may be based on physical principles as well as observations, and they can be classified as empirical, semi-empirical or theoretical (Tedesco and Kim 2006).

Having a model that is capable of predicting the observed radiation with the required accuracy, the next step will be to invert the model in order to predict snow variables from the observed radiation. Such inverted models can be used in snow variable algorithms. The model inversion requires some assumptions to be done, like fixing some of the model parameters or snow variables. The inversion if the radiation model will typically involve non-linear inversion techniques (see Pardé *et al.* 2007). The inverting problem will in practice be solved only for fairly simple (semi-)empirical radiation models, while theoretical radiation models are not feasible for geophysical inversion (Pulliainen *et al.* 1999).

Relationships between EM quantities and snow variables that are obtained from observations only, are referred to as empirical models (Tedesco and Kim 2006). They are closely related to the snow signatures described in the section above. The retrieval of snow variables from these models is fast, but the validity of the models is geographically limited.

Theoretical radiation models are developed independent from empirical data and are based on physical theory only. Models like the dense medium radiative theory (DMRT) and the strong fluctuation theory (SFT) have been widely used to simulate the brightness temperature of snow (Tedesco and Kim 2006). The DMTR model considers a dense medium, i.e. a medium where the particles occupy more than 10% of the volume. When the distance between the grains becomes shorter than the wavelength, the scattering from one snow grain will no longer be independent of that from another grain. Several solutions to this problem exist in the literature (see Tedesco and Kim 2006). The SFT model considers a continuous medium where scattering is explained by random permittivity fluctuations, which are modelled by a correlation function. The strong fluctuations in SFT mean that the correlation function has a large variance. In both the methods the calculation of the brightness temperature involves Gaussian quadrature methods and eigenvalue calculations.

Semi-empirical models refer to models that are developed by combining theory with empirical results. The two most common models are the HUT model (Pulliainen *et al.* 1999) and the MEMLS model (Wiesmann *et al.* 1998).

The HUT model was developed at the Helsinki University of Technology TKK (**T**eknillinen **k**orkea**k**oulu), recently also referred to as the TKK model (e.g. Tedesco and Kim 2006). The model is based on radiative transfer theory and uses a semi-empirical emission model for a homogeneous snowpack. Effects caused by the atmosphere, forest cover, and the soil surface are modelled separately by empirical approaches and included in the total model.

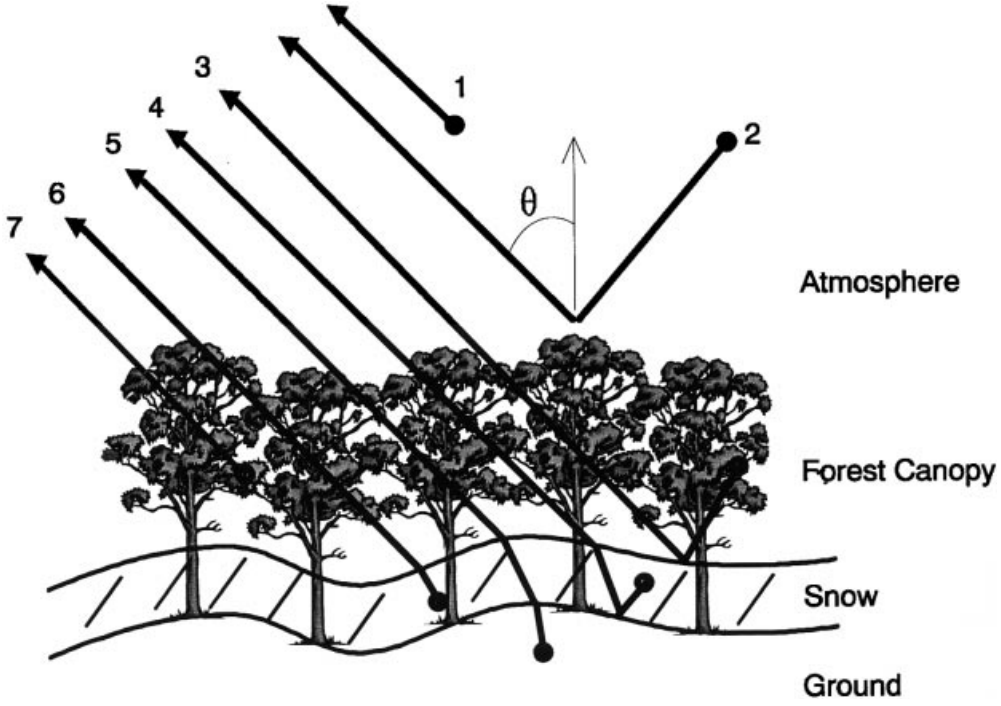

Figure 4.2. The HUT model considers emission and scattering in one snow layer and a few other layers. These layers are the soil, the vegetation and the atmosphere.

The snow variables that influence the emission from the snow, include snow depth (SD), grain size (SGS), snow temperature, and wetness. For wet snow the surface roughness is also relevant. The model considers two interfaces, one between snow and air and one between snow and soil, but no internal layering. Its basic assumption is that forward scattering dominates. Pulliainen *et al.* (1999) also tested how the inversion of the HUT model could be used for the estimation of SSW, and found that the model approach was less biased than empirical approaches. This means that is has a larger potential for being more useful for large scale applications. The details concerning the model formulation and its inversion are given by Pulliainen and Hallikainen (2001).

Studies undertaken by Wiesmann *et al.* (1998) initiated the MEMLS model. In these studies the emission from dry snow was measured in various frequencies and then compared with two radiation models. While a two-flux radiation model was too simple, a six-flux model showed good correspondence between the modelled and the measured absorption coefficients, which are independent of snow type. The scattering coefficients depended on frequency and grain size.

The MEMLS model (Mätzler and Wiesmann 1999; Wiesmann and Mätzler 1999) considers the snowpack as a stack of horizontal, planar layers with individual values for thickness, grain size (correlation length), density, wetness, and temperature. This sandwich model combines the scattering and refraction at the interfaces by means of multiple-scattering radiative transfer theory. The volume scattering within the layers is modelled by combining a two-flux approach (upwelling and downwelling fluxes) and a six-flux approach. The absorption depends on the temperature, the scattering depends on the correlation length (grain size), and both of them depend on the density and frequency.

A snow pack may vary in many characteristics, which is difficult to measure and quantify. A classification system for seasonal snow (Sturm *et al.* 1995) defines its classes by an ensemble of snowpack characteristics: stratigrafy, thickness, density, crystal morphology, and grain characteristics. The system has these six classes: prairie, tundra, taiga, alpine, maritime, and ephemeral. Tedesco and Kim (2006) examined the semi-empirical HUT (referred by them to as TKK) and MEMLS models and the theoretical DMRT and SFT models, by comparing them to each other for all six snow types. They found that the models differed significantly with respect to their resulting brightness temperature and extinction coefficients. None of the models were able to reproduce the experimental data systematically.

Mätzler *et al.* (2006) discuss microwave emission from snow and argue that physical modelling is needed. In general they recommend both the HUT model and the MEMLS model. The HUT model includes emission contributions from the vegetation and atmosphere, which enables the interpretation of satellite microwave radiometer data. The HUT emission model is sufficiently simple to be inverted for the direct retrieval of SWE in simple snowpacks, but the model does not account for strong vertical gradients. The MEMLS model is more complex and not suitable for direct retrieval of snow variables. However, it will be a good reference source for the construction of simpler, invertible models for snow variables.

Table 4.2. *Types of microwave radiation models for snow*

Model type	Advantages	Disadvantages
Empirical	Fast and direct retrieval	Limited validity, must rely on assumptions on
Semi-empirical	Possible to include in retrieval algorithms	Not so fast
Theoretical	Well based on physical principles. Useful for validation and simulation	Difficult to include in retrieval algorithms

Table 4.3. *Specific radiation models for snow*

Model	Model type	Characteristics
HUT	Semi-empirical	Considers one homogeneous snow layer Includes soil, vegetation and atmosphere.
MEMLS	Semi-empirical	A sandwich model that considers a layered structure of the snow pack. Too complex for retrieval algorithms, but useful for their validation
DMRT	Theoretical	Models the snow pack as a medium consisting of scattering particles (the snow grains) packed so closely that the scattering no longer is independent
SFT	Theoretical	Models the snow pack a continuous medium with random inhomogeneities

5 Algorithms

Algorithms for snow variables may be retrieved from simple snow signatures, they may be the outcome of analyzing and running models, or they may directly involve model runs, or model inversions.

Methods to detect global snow cover are well advanced and have been applied routinely at various scales. Methods to retrieve SWE or snow depth are not mature, and they have a tendency to underestimate the snow volume in more complex settings (Kelly and Chang 2003).

5.1 Snow cover extent

The snow cover can be d etected directly by separate algorithms (e.g. Mätzler 1994), but may also be retrieved by first estimating the snow depth or water equivalent and then using a threshold on that value. In the latter case a more direct snow cover algorithm may easily be defined, if required.

The spectral gradient is used in most algorithms for snow cover detection. Künzi *et al.* (1982) used the spectral gradient method on SMMR data to map snow cover extent and found that the resulting line delimiting the snow cover corresponded to 5 cm snow depth. Snow cover was defined by the threshold:

$$(T_{18H} - T_{37H}) > 3.8 \text{ K}$$

Snow was not detectable when being in wet condition, but by taking the minimum spectral gradient over repeated acquisitions, dry snow were found. McFarland *et al.* (1987) used a spectral gradient approach on data from SMMR and found that it was possible to detect snow cover with a few cm thickness.

Chang at al. (1987) applied a threshold of 1.6 K in their SWE algorithm. They found that the resulting snow covered area was 10% less than their reference data. This difference was explained by the penetration capability of the microwaves, leaving snow covers thinner than 5 cm undetected. Also Goodison (1989) applied a threshold on SWE estimates, and recommended the spectral gradient method on vertically polarized SSM/I data, without supplying any coefficients.

Hallikainen (1989) applied vertically polarized data and used the spectral difference ($T_{18V} - T_{37V}$) for snow-free conditions as a reference. The threshold was tested against the change in the spectral difference. Different thresholds were used for southern Finland (9.7 K) and northern Finland (12.5 K)

Nagler (1991) took advantage of the 89 GHz band in SSM/I and included the new spectral difference ($T_{37H} - T_{89H}$) in addition to ($T_{18H} - T_{37H}$). The new feature was more sensitive to thin snow.

Mätzler (1994) examined spectral emissivity signatures for many relevant surface types in order to separate snow from non-snow in various areas. Open waters were identified by low emissivity in 10 GHz ($\varepsilon_{v10} = 0.5$), while other snow-free areas were identified by low

values in an index that is a combination of polarisation differences at various frequencies and the spectral gradient at vertical polarisation:

$$comb = \varepsilon_{v10} - \varepsilon_{h10} + \varepsilon_{v21} - \varepsilon_{h21} + \varepsilon_{v35} - \varepsilon_{h35} + 3(\varepsilon_{v10} - \varepsilon_{v35})$$

The combined index will have values <0.1 for snow-free areas, and typically ca. 0.7 for snow. Note that the snow class will contain both dry and wet snow. One problem is that powder snow will often have low values, like non-snow. High frequency microwaves (96 GHz) may identify powder snow if we ignore the effects of the atmosphere.

Hiltbrunner (1996) also suggested a combined emissivity algorithm for SSM/I data:

$$comb = \varepsilon_{v19} - \varepsilon_{h19} + \varepsilon_{v37} - \varepsilon_{h37} + 3(\varepsilon_{v19} - \varepsilon_{v37}) > 0.14$$

Grody and Basist (1996) developed a decision tree algorithm for global snow cover mapping from spectral gradients in SSM/I data. The algorithm utilizes the high-frequency channels of SSM/I in order to detect thin snow cover, but need also low-frequency channels to separate snow from atmospheric effects as precipitation. The design of the decision tree is based on empirical relationships between SSM/I data and various snow-free surface conditions. The outline of the algorithm is like this:

- Identify potential snow : $T_{22V} > T_{85V}$ OR $T_{19V} > T_{37V}$
- Eliminate precipitation, incl. cold rain and deep convection
- Eliminate cold deserts
- Eliminate frozen ground covered by sparse vegetation
- Include glacial ice (Greenland and Antarctica)

The algorithm showed good agreements with digitized show charts from NOAA, which are based on visual interpretation of AVHRR images. However, the thinnest snow packs (<2.5cm) were missing. Furthermore, melting and wet snow were not detected, as attempts to identify these snow types lead to confusion with atmospheric precipitation. Instead, the classification was undertaken on night time acquisitions. The microwave data had a tendency to yield less snow than present under problematic conditions, like melting or thin snow, under dense forest, and during precipitation events. In addition, frozen ground could be classified as snow. The frozen ground detection was improved by Tait *et al.* (2001).

Armstrong and Brodzik (2002) compared several passive microwave snow algorithms (Chang *et al.* 1987; Goodison 1989; Nagler 1991; Grody and Basist 1996). They reported that all of them yielded less snow than NOAA Northern Hemisphere snow charts derived from manual interpretation of visible satellite data, like AVHRR. The underestimation in early winter were explained by the thin snow cover, where optical data seems to be able to detect thinner snow than does microwave data, 2 cm vs. 5 cm. Higher frequencies are expected to be more sensible to thin snow cover, but will also face more problems related to atmospheric attenuation.

The decision tree approach of Grody and Basist (1996) has been developed further by incorporating more data into the analysis (Tait *et al.* 2000). In addition to the results retrieved from SSM/I the input data set include the digital show chart from NOAA, snow depth data

from climate stations, and surface elevation data. The classification added two categories for snow states between snow-free and completely snow-covered. Although many of the problems associated with SSM/I data alone were solved, boreal forests were still problematic. Tait *et al.* (2001) suggested incorporating AMRS as a supplement in the algorithm for making the MODIS snow cover product.

The AMSR-E Snow Water Equivalent algorithm (Chang and Rango 2000) follows the outline of Grody and Basist (1996) for the identification of dry snow cover. Wet snow is detected according to Walker and Goodison (1992).

In a study of the duration of snow cover in northern Canada Brown *et al.* (2007) applied a threshold of 1 cm on SWE retrieved from SSM/I data by means of the Environment Canada open environment SWE algorithm: $SWE = -20.7 + 2.59\ (T_{19H} - T_{37H})$.
Their retrieval of SWE in the tundra regions was very uncertain due to large vertical gradients in the snow pack and a complex subpixel snow cover distribution, but microwave radiometry is still adequate for capturing the snow cover and its temporal variability.

Kärnä *et al.* (2007) used the horizontally polarised spectral gradient between 19 and 37 GHz for detecting dry snow:

- First estimate snow depth as $D = 15.9(T_{19H} - T_{37H})$
- Snow covered if $D > 80$ mm AND $T_{19H} < 250$ K AND $T_{37H} < 250$ K

Wet snow

While dry snow is detected because it scatter the upwelling radiation and thus reduce the brightness temperature, the detection of wet snow must rely on other means. Walker and Goodison (1992; 1993) considered the polarization difference at 37 GHz for SSM/I, and found that this difference was higher for wet snow than for open snow-free prairie areas. The polarization difference is assumed to increase for lower frequencies.

5.2 Snow depth and water equivalent

From a physical point of view, it is the snow water equivalent (SWE) that is the snowpack bulk property that influences the microwaves directly (Kelly *et al.* 2003). Assuming a standard snow density of 0.3 kg/dm^3 (Chang *et al.* 1987), conversions between SWE and the snow depth (SD) can be obtained. By convention SD is quantified in cm and SWE in mm, and the conversion factor can thus be formulated as 3 mm/cm.

Empirical algorithms

Until 10 years ago, the main focus was on developing empirical algorithms for SWE or SD. Due to practical consideration concerning training and validation data, these algorithms are based mostly on SD observations.

Künzi *et al.* (1982) suggested an algorithm for retrieving snow depth from SMMR data, supposed to be valid in the range between 5 cm and 50 cm. This algorithm, which has been referred to as the NASA Goddard algorithm (see Solberg *et al.* 1997), is given by:

$$SD = (T_{18H} - T_{37H}) * 1.46\ \text{cm/K} + 2.46\ \text{cm}$$

Computed snow signatures (Chang 1986) were used to derive a simple spectral gradient algorithm for retrieving the snow depth from SMMR data (Chang *et al.* 1987). It uses the spectral gradient between the frequencies 18 and 37 GHz, horizontally polarized. The algorithm is supposed to be valid in the range between 2.5 cm and 100 cm and is given by

$$SD = (T_{18H} - T_{37H}) * 1.59 \text{ cm/K}.$$

The scaling factor corresponds to a grain size of 0.3 mm and a density of 0.3 kg/dm^3. Assuming the same density, the SWE is given by (Chang *et al.* 1987)

$$SWE = 4.8 \text{ mm/K} * (T_{18H} - T_{37H})$$

SWE values derived from SMMR data with this algorithm were found to correspond well with available snow depth data in uniform, flat areas (like Canada, Russia), but forests and mountains were problematic (Chang *et al.* 1987). Tait and Armstrong (1996) did also apply the algorithm of Chang *et al.* (1987) for retrieving the snow depth from SMMR data. Armstrong and Brodzik (2001) modified the algorithm for retrieving snow depth from SSM/I antenna temperatures. The snow depth is given by $d = 1.59 \text{ cm/K} * (T_{19H} - 6\text{K}) - (T_{37H} - 1\text{K})$.

In order to account for variations in the underlying ground Hallikainen and Jolma (1986) suggested relating SWE to the difference in the brightness temperature between a snow-free state and the snow-covered state under consideration. Empirical studies in Finland applying SMMR data (see also Hallikainen and Jolma 1992) showed that only the 37 GHz frequency was in agreement with SWE observations. However, compared to the 37 GHz brightness temperature, signature functions including an additional lower frequency improved the accuracy of the retrieved SWE, e.g. $T_{18H} - T_{37H}$ (see Hallikainen 1984). Vertically polarized data performed somewhat better than horizontally polarized data.

In a more close examination of the spectral difference $T_{18V} - T_{37V}$, Hallikainen (1989) found different regression coefficients for Southern and Northern Finland, and explained it by the differences in vegetation coverage. In a later study Hallikainen and Jolma (1992) included $T_{10V} - T_{37V}$, and found that the two had about the same overall performance. The best correlation was obtained in Northern Finland with $T_{10V} - T_{37V}$. Northern Finland has deeper snow and less forest cover than Southern Finland.

McFarland *et al.* (1987) examined the polarization difference in data from the SMMR instrument and found that it was linearly dependent of snow depth up to 15 cm. The difference performed best at shorter wavelengths.

Aschbacher (1989) combined the spectral difference in vertical polarization with the polarization difference to obtain a more robust feature. Linear regressions were then made for SMMR and SSM/I. The spectral-polarization difference (SPD) is defined as:

$$SPD = (T_{18V} - T_{37V}) + (T_{18V} - T_{18H})$$

and the regression functions are (see Solberg *et al.* 1997):

- $SWE = 2.2 \text{ mm/K } SPD - 7.11 \text{ mm}$ (SSMR)
- $SD = 0.68 \text{ cm/K } SPD - 0.67 \text{ cm}$ (SSMR)
- $SD = 0.79 \text{ cm/K } SPD - 7.01 \text{ cm}$ (SSM/I)

Pulliainen (2006) used the SPD in linear regression functions as a baseline algorithm.

Mätzler (1994) reported that even if one considers dry winter snow, no accurate inversion algorithm exists for retrieving the SWE from microwave radiometry. The problems will increase when the snowpack is a mixture of snow types. He suggested a combination of polarisation and spectral gradients.

Table 5.1 . *Retrieval functions for 16 snow categories (after Tait 1998). The snow categories were defined according to their forest cover, terrain complexity, snowmelt, and depth hoar. The retrieval functions are linear combinations of spectral/polarization differences among 19 GHz, 37 GHz, and 85 GHz, vertically and horizontally polarization.*

	Category	Retrieval function
1	Nonforested, noncomplex, no melting snow, no depth hoar	$SWE_1 = 12.9 + 3.1(19H–37H)$
2	Nonforested, noncomplex, melting snow, no depth hoar	$SWE_2 = -7.3 + 6.6(19H–37H)$
3	Nonforested, noncomplex, no melting snow, depth hoar	$SWE_3 = 98.8 + 0.8(19V–37H) + 2.6(19H–85H) - 1.2(19V–85V) - 3.2(19H–85V)$
4	Nonforested, noncomplex, melting snow, depth hoar	No analysis for Category 4: insufficient data
5	Forested, noncomplex, no melting snow, no depth hoar	$SWE_5 = 26.4 - 1.3(19V–37H)$
6	Forested, noncomplex, melting snow, no depth hoar	$SWE_6 = 26.362 - 7.1(19H–37V)$
7	Forested, noncomplex, no melting snow, depth hoar	$SWE_7 = 110.4 + 2.7(19H–85H) - 3.9(19H–85V)$
8	Forested, noncomplex, melting snow, depth hoar	$SWE_8 = 20.3 + 5.4(19V–37V)$
9	Nonforested, complex, no melting snow, no depth hoar	$SWE_9 = 32.0 + 12.9(19H–37H)$
10	Nonforested, complex, melting snow, no depth hoar	$SWE_{10} = 140.7 + 12.7(19H–37H)$
11	Nonforested, complex, no melting snow, depth hoar	$SWE_{11} = 405.0 + 6.6(19H–37H) - 11.3(19V–37H)$
12	Nonforested, complex, melting snow, depth hoar	$SWE_{12} = 320.32 - 5.0(19H–37H)$
13	Forested, complex, no melting snow, no depth hoar	$SWE_{13} = 50.0 + 82.7(19H–37V)$
14	Forested, complex, melting snow, no depth hoar	$SWE_{14} = -285.8 + 61.4(19H–37V) + 26.2(19H–85V) + 50.8(PW)$
15	Forested, complex, no melting snow, depth hoar	$SWE_{15} = 470.9 - 14.6(19V–37V) + 28.8(19V–37H) + 23.1(19H–85H) - 34.4(19V–85H)$
16	Forested, complex, melting snow, depth hoar	No significant model for Category 16

***Table 5.2**. An overview of some empirical algorithms for SD, SWE, and SE*

Algorithm	Year	Instru-ment	Snow depth	SWE	Snow extent	Approach	Comments
Künzi	1982	SMMR	SD		SE	Spect. diff.	NASA Goddard algorithm
McFarland	1987	SMMR	SD		SE	Spect. diff.	
Chang	1987		SD	SWE	(SE)	Spect. diff.	The classical one
Goodison	1989 1990	SSM/I		SWE	(SE)		Canadian prairies algorithm
Hallikainen	1989	SSMR		SWE	SE	Spect. diff.	Differ. btw. North and South Finland
Aschbacher	1989	SMMR SSM/I	SD	SWE		Spectral-polarization diff	Several regression functions
Nagler	1991	SSM/I			SE	Spect. diff.	
Hallikainen & Jolma	1992	SMMR		SWE		Spectral diff compared to bare ground	
Mätzler	1994	SMMR		SWE	SE	Emissivity combinations	Multi-frequency and polarization
Hiltbrunner	1996	SSM/I			SE	Emissivity combinations	
Grody and Basist	1996	SSM/I			SE	Decision tree	
Tait	1998	SSM/I		SWE		Spect. diff. / Decision tree	
Chang and Rango	2000	AMSR-E		SWE	SE	Decision tree	
Armstrong & Brodzik	2001	SSM/I	SD			Spect. diff.	Modific. of Chang
Tait	2001	SSM/I			SE	Decision tree	Dev. from Grody & Basist
Brown	2007	SSM/I			SE	Spect. diff.	
Kärnä	2007	SSM/I			SE	Spect. diff. & other	SE derived from SD and other features

Tait (1998) examined 16 snow categories, defined by their characteristics with respect to snow wetness, depth hoar, terrain, and forest density. Empirical functions between SWE and SSM/I data were established for each of them, as shown in Tab. 5.1.

Singh and Gan (2000) gave an overview of some empirical algorithms developed during the 90ies, and suggested additional two. These include:

- SWE = -20.7 mm + 2.59 mm/K ($T_{19V} - T_{37V}$) (Goodison *et al.* 1990)
- SWE = -25.0 mm + 4.8 mm/K ($T_{19H} - T_{37H}$) (1-A_F) (Chang *et al.* 1996)
- SWE = -108.7 mm + 8.7 mm/K [($T_{19H} - T_{37H}$) - ($T_{19H} - T_{37H}$)$_{\text{snow-free}}$] - North Finland
  SWE = -98.0 mm + 10.1 mm/K [($T_{19H} - T_{37H}$) - ($T_{19H} - T_{37H}$)$_{\text{snow-free}}$] - South Finland
  (Halllikanen 1989)
- SWE = 2.34 mm/K ($T_{18H} - T_{37H}$)/(1-A_F) (interior Eurasia)
  SWE = 4.77 mm/K ($T_{18H} - T_{37H}$)/(1-A_F) (elsewhere) (Foster *et al.* 1997)
- SWE = 0.2357($T_{19V} - T_{37H}$) + 0.0064 Z + 4.04(1-A_F) – 0.029(1-A_W) + 1.0825 TPW
  SWE = 0.168($T_{19V} - T_{37V}$) + 0.0052 T_{19H} – 0.0028 Z + 11.99 A_F (Singh and Gan 2000)

In these algorithms, A_F represents the forest fraction of the cell, A_W represents the water fraction of the cell, Z is the cell mean elevation, TPW is atmospheric water vapour. An important finding for all these algorithm is that it was necessary to add a shift parameter, i.e. adjust the offset, in order to obtain good validation results (Singh and Gan 2000).

The Canadian prairies algorithm for SWE (Goodison *et al.* 1990), is based on SSM/I measurements, and has been operational in Canada since 1990. It was later updated to forested areas (Derksen *et al.* 2002 ; Goïta *et al.* 2003). The algorithm calculates SWE differently for different cover types, and for mixed cells the SWE is calculated as a weighted sum of cover specific SWE values. The algorithm is based on the spectral gradient: $SG = T_{37V} - T_{19V}$, and the cover specific SWE values are given by (Derksen *et al.* 2005a):

- Open areas: SWE = –20.7 mm – 2.59 mm/K SG (the original prairies algorithm)
- Sparse forest SWE = –1.95 mm – 2.28 mm/K SG
- Conif. forest SWE = 16.81 mm – 1.96 mm/K SG
- Decid. forest SWE = 33.50 mm – 1.97 mm/K SG

These formulas have shown to yield good results, even in areas with depth hoar (Goïta *et al.* 2003).

Snow depth from the temperature gradient

The spectral gradient is dependent not only on the snow depth / SWE, but also on the snow grain size. One of the implications of this is that empirical relationships between SWE and spectral gradient may vary form year to year, depending on the state of the snow pack.

In a study covering the Northern Great Plains of America during the 1988/89 season Mognard and Josberger (1998) observed a strong increase in the spectral gradient during the coldest part of the season, when there was no significant snowfall. This was explained by a rapid increase in snow grain size into depth hoar, due to strong snow metamorphosis under cold conditions. They suggested the accumulated temperature gradient index,

$TGI = \sum(-T_{air} / D) / C$, as an index of the metamorphosis (Josberger and Mognard 1998). The constant C = 20K/m is a scaling factor, referred to as the critical temperature gradient. Strong correlations between TGI and the spectral gradient $SG = T_{19H} - T_{37H}$ were found for early parts of the accumulation seasons.

The TGI index was developed further in order to integrate the snow grain size into a snow depth retrieval algorithm (Josberger and Mognard 2002). Assuming a strong correlation between the spectral gradient and TGI, the latter can be estimated from the former. It should then be possible to estimate the current temperature gradient by examining the change in the TGI estimate during a suitable time interval. In order to avoid short time fluctuations, the interval shouldn't be too short. The temperature gradient is the temperature difference between the top and bottom of the snowpack, divided by the thickness of the snowpack, i.e. the snow depth. The snow depth can now be found as

$$D = \frac{-\alpha(T_{air} - T_{bottom}) / C}{SG - SG_0 \big/ t - t_0}$$

The spectral gradients SG and SG_0 are observed at time t and t_0, respectively. T_{air} is the current (t_0) air temperature, while T_{bottom} can be assumed to be constantly 0 °C. The coefficient α is determined from the correlation between the spectral gradient and TGI.

In a study of Central Siberia, Grippa *et al.* (2004) adopted the algorithm to account for ground temperatures below 0 °C by using bottom temperature values derived from permafrost data. The coefficient α was set to 3.5, independent of time and location. Soil temperature models have also been applied for the improvement of the ground temperature input to the algorithm (Boone *et al.* 2006).

The dynamic TGI algorithm requires that the spectral gradient must change in time (Grippa *et al.* 2004). This will happen during rapid crystal growth in early winter, when the snow cover is thin and the air is cold. When the temporal change in the spectral gradient falls below a threshold, the algorithm cannot be used since it may overestimate the snow thickness. An alternative is to use the static algorithm $SD = a\,SG$ (see Chang *et al.* 1987).

Grippa *et al.* (2004) therefore suggested a combined approach starting with the dynamic TGI algorithm, but changing to the static algorithm after reaching a threshold of 0.2K/day, which is expected mid-way through the season in Siberia. The coefficient a in the static algorithm is adjusted to match the snow depth results from the dynamic algorithm. The coefficient will consequently vary in space.

Biancamaria *et al.* (2008) assessed the performance of the dynamic algorithm, as proposed by Grippa *et al.* (2004), and suggested a modification of it, referred to as the extended dynamic algorithm. One problem of the dynamic algorithm is that some areas are below the 0.2K/day threshold also in the beginning of the season. These areas needed to initiate the coefficient a, which was done by fitting the static algorithm (see Chang *et al.* 1987) to observations of SD and SG for January.

The assessment examined the static algorithm, the dynamic algorithm and the extended dynamic algorithm for the Northern Hemisphere and compared their results with GSWP-2 snow depth data. The static algorithm did not work well, as results for January were

uncorrelated with the reference and the snow rich areas were located incorrectly. The two dynamic algorithms located the maximum snow depth areas correctly and showed positive correlations (0.5-0.6) with the reference data. The results were better over Eurasia than over North America, and it was suggested that this was because of the higher density of lakes in the latter region. In general the spectral gradient from lakes will be opposite of land snow even if the lakes are covered by ice or snow.

Dynamic models for the snow grain size

Empirical models for the evolution of grain size and density have been found by using time-invariant data from weather stations (Kelly *et al.* 2003). The models are used for computing the spatial pattern of the coefficients in the spectral difference algorithm. Kelly *et al* (2003) combined dynamic grain size estimates with the DMRT model in order to retrieve SWE. The development of the grain size as well as the density was modelled by means of the temperature gradient, where the surface temperature was estimated as a linear regression of a set of brightness temperatures. Note that this way of relating the grain size to the temperature gradient could be considered as the opposite of the TGI approach of Mognard and Josberger (1998), who first estimated the grain size development and then retrieved the temperature gradient.

Foster *et al.* (2005) defined a time dependent correction parameter for a set of given snow classes (see Sturm *et al.* 1995). In that way they obtained an algorithm that made systematic error corrections depending on the factors like vegetation cover and snow morphology.

The NSIDC algorithm

The National Snow and Ice Data Center (NSIDC) in USA delivers SWE products retrieved from microwave radiometer data. The algorithm is based on spectral difference methods described by Chang *et al.* (1987; 1997). Enhancements have been made in the new algorithm (Kelly and Foster 2005; Kelly *et al.* 2005).

The algorithm requires some ancillary data (http://nsidc.org/data/docs/daac/ae_swe_easegrids.gd.html):

- Forest density (GLCF_MODIS_VCF)
- Forest fractional cover (MOD12Q1 / IGBP classification)
- Snow density (ground stations)
- Land mask (MOD12Q1)
- Snow possibility mask

The algorithm follows this outline:

- Identify where snow is possible
- Identify dry snow cover (Kelly et al. 2003),
- Retrieve snow depth (SD), separately for forest and non-forest
- Aggregate SD to EASE-grid cell
- Convert SD to SWE, using ancillary snow density

- The aggregated versions (5-days and 1 month, respectively) of the SWE product are obtained from the daily products by taking the maximum SWE value

Utilization of weather station data

Kelly and Chang (2003) examined the relationship between the vertically polarized spectral difference $T_{18V} - T_{37V}$ and SWE observed at weather stations covering he Northern Hemisphere. For each station linear regression coefficients were estimated, and a unique SWE formula thus obtained. A spatial model of the coefficients in the SWE algorithm was then obtained by spatial interpolation of the regression coefficients between the station localities. Kriging was used for the spatial interpolation. It appeared to be some relationship between the coefficients and the forest cover fraction. The effects of the forest cover fraction were studied more closely by considering the estimation bias of the new algorithm, and using the forest cover for explaining the bias. A correction factor that could be retrieved form a forest cover fraction maps was suggested. In a comparison with the original spectral difference algorithm of Chang *et al.* (1987), the final algorithm showed to be more accurate. The accuracy of the algorithm decreased during the winter, most likely because of the uncertainty related to the grain size development.

Snow depth from the HUT model

An operational system for the production of SWE over the whole Eurasia is described by Kärnä *et el.* (2007). The snow depth (SD) and water equivalent (SWE) are here retrieved from the spectral gradient between vertically polarized 18.7 and 36.5 GHz brightness temperatures from EOS AMSR-E data. In addition, the polarisation difference at 18.7 GHz may be used. Note that this polarisation differs from what was used in their snow cover detection described above. The HUT model, which predicts the spectral gradient from a set of snow variables, is inverted by means of a Bayesian inversion method.

The most important inputs to the HUT model are the snow water equivalent and the snow grain size. In addition it needs the depth, density, and temperature of the snow, as well as soil properties, canopy characteristics, and the atmospheric contributions to emission and transmission. In order to invert the HUT model, one needs to consider the snow grain size as well as the snow depth.

An inversion algorithm for the HUT emission model was suggested by Pulliainen and Hallikainen (2001). The grain size and the SWE (or SD) are retrieved in an iterative procedure that aims at minimizing the differences between observed and modelled quantities. These quantities are typically some spectral difference or a polarisation difference. More specifically, the applied gradients are the spectral difference between 19 and 37 GHz vertically polarized, and the polarisation difference in 19 GHz. It is assumed that the model prediction errors as well as the grain size values are normally distributed. Finally, the temporal variation of snow depth may be included in the optimization, i.e. a former estimate of SD can be used as a third reference.

The inversion algorithm has been developed further (Pulliainen 2006) into an assimilation algorithm. Here the grain size is not considered as a free variable, but is estimated from weather station data. By using snow depth measurements from the stations, a grain size value for each station can be retrieved from the HUT model. This is done by letting the grain size be the fitting parameter for the minimization of the difference between the

observed and the modelled spectral gradient. Grain size values are then retrieved for each cell as a block average of the closest stations. The weather station data is also used for getting prior estimates for the snow depth. A prior estimate for each cell is estimated by ordinary Kriging of the weather station data. This interpolation method takes into account the spatial autocorrelation of snow depth, including the degree of correspondence between point data and regional averages as seen from the satellite. The last step of the algorithm aims at minimizing the differences between observed and modelled values for the spectral gradients, as well as the difference between estimated and prior values of the snow depth. As for the optimization algorithm, the temporal variation of snow depth may be included in the assimilation. The main steps of the algorithm are:

For each of the weather stations:

- Observe snow depth
- Observe satellite microwave data
- Estimate grain size using the HUT model

For each cell in the grid:

- Interpolate grain size
- Interpolate snow depth
- Get spectral gradient form satellite data
- Get modelled spectral gradient
- Get modelled snow depth from inverting the HUT model
- Get snow depths history
- Minimize model deviations

To summarize, in the assimilation method the satellite data as well as the interpolated ground-based data are weighted according to their spatial and temporally varying statistical accuracy (Pulliainen 2006). The system is operated by the Finnish Meteorological Institute (FMI). It is implemented in Matlab and runs on a *linux* platform. Satellite and weather station data are downloaded automatically. Water areas are masked out.

The method has been demonstrated for Eurasia for spring 2007 and has been validated by Pulliainen (2006). The validation showed an RMS error of 12-18 cm for snow depth estimations in four test regions in Eurasia. However, the validation showed that the results reached saturation for deep snow. The algorithm was also applied on SSM/I data from four winters in Northern Finland, and yielded RMS errors of 23-58 mm, which improved to 17-28 mm when mid-winter only was considered.

Pardé *et al* (2007) used the HUT model for retrieving SWE and grain size in Canada. Both snow variables were retrieved simultaneously. Their suggested technique for inverting the HUT model requires initial values for the requested variables, which were available from meteorological stations. The experiment included airborne campaigns as well as field data. The precision depends on the location and on the winter season, but has a global precision of about 25 mm. When there was little snow, SWE was overestimated.

5.3 Discussion

The microwave signature of dry snow depends on many characteristics of the snow pack, including amount of snow, grain size, and layering. These effects are difficult to separate from each other. Current research is focusing on modelling the microwave emission from snow and how to invert these models into retrieval algorithms for snow variables. Serious problems are related to the complexity of the snow pack.

Snow cover, snow depth, and snow water equivalent (SWE) are all correlated to each other. From a physical point of view the SWE, which represents the amount of snow, will be most directly linked to the microwave signal, because it is the total attenuation from the snow to the signal emitted from the underlying ground that is measured.

Some approaches address snow depth (SD), while others address snow water equivalent (SWE). It is not always clear why the one is chosen instead of the other, but it may be related to which of the two snow variables that is available during an experiment. From a physical point of view we should prefer to predict SWE from the spectral gradient, but from a more practical point of view it may be more convenient to consider SD data when they are available from weather stations. The two quantities are highly correlated and their relation to each other is determined by the snow density. It should therefore be possible to convert between the two quantities.

Empirical relationships between SWE and snow signatures have thus been frequently reported in the literature, but valid only within constrained conditions. Snow depth (SD) has been related to snow signatures in a similar way. The estimated values for SWE or SD are assumed to be some average for the resolution cell. This makes sense from a physical point of view, but only up to a certain snow depth which depends on the frequency. Deep snow tends to be underestimated, due to the non-linear relationship between the scattering and the amount of snow.

Retrieval of the snow cover is less difficult, and is typically undertaken by first estimating the snow thickness, in terms of cm snow or as SWE, and then using a threshold for the classification of each pixel as snow or snow-free. Alternatively the snow cover is retrieved by applying a threshold directly on the spectral gradient, which may differ somewhat from the gradient used for SWE estimation.

Snow detection

Inside a resolution cell there will be variations in snow depth. For thin snow-packs, this variation will be closely related to the patchiness of the snow. A cell classified as snow may very well contain snow-free patches, and *vice versa*. In such cases the choice of threshold is very important. The concept of snow-free / snow-covered is related to the snow-cover fraction. The limit could be defined as 50% snow cover, or at any other snow fraction.

However, because the microwaves penetrate through the snow pack, their signature is ruled by the snow volume, and not by its area. The threshold used for the separation between snow and non-snow is therefore coupled to the average snow depth, and not to the areal fraction of snow. The relationship between area and volume may vary, and depend on how the snow is distributed within the cell. Jiang *et al.* (2007) accordingly state that "In global SWE monitoring, the sub-grid heterogeneity is expected to have significant

impact and has to be taken into account". As long as the distribution of the snow within a cell is unknown, it is difficult to estimate the snow cover with any certainly.

For a given snow cover limit for the categorization, there will be several uncertainties. Firstly, the coupling between snow cover and snow volume is described above. Secondly, the accuracy of the volume estimate from the observed microwave signal must be considered. Even if a direct algorithm is applied, it is based on these principles.

When snow thickness increases, the uncertainties related to the snow detection will be significantly reduced. However, then the uncertainties with respect to SWE will increase, in particular when the snow pack has a layered structure.

Wet snow is very different from dry snow. It behaves like dry or frozen ground, emitting its own radiation, and absorbing the radiation from the ground and the internal layers in the snow pack. Microwaves are sensitive to small amounts of liquid water content, but will quickly reach a saturation level (Tedesco *et al.* 2006). Methods exist for the detection of wet snow, but any attempt to estimate of the amount of snow will fail.

Effects of snow grain size

In addition to SWE or SD, the spectral gradient is also dependent on other snow variables. The most important one is the snow grain size, which in some cases will dominate the SWE with respect to the spectral gradient. It is therefore very important to consider the grain size in SWE/SD retrieval algorithms, and correct for its effects.

The TGI approach is developed for the estimation of SD in areas with a cold, continental climate, i.e. those parts of the world where the winter can be described as vey cold and with little precipitation. Under these conditions the snow grains will grow rapidly due to large vertical temperature gradients in the snow pack. The temporal development of the spectral gradient is therefore dominated by the growth of the snow grains. One paradox is that the spectral gradient therefore may be larger in areas with the thinnest snow, which contradicts what is common in other regions.

The TGI algorithm considers the temporal change in the spectral gradient and assigns this change solely to the growth of the snow crystals, ignoring any snow accumulation that may have taken place. Furthermore, it seems that the direct effects of SWE on the spectral gradient are ignored when the linear regression function between TGI and the spectral gradient is determined. Behind the linear regression coefficient α there exists thus an implicit assumption of a certain SWE, which is not necessarily in accordance with the SD value retrieved from the algorithm. It is very unclear how spatial variations in SWE will influence the relationship between TGI and the spectral gradient, but it is obvious that some errors will be introduced. How these errors will propagate to the final estimate of snow depth should be investigated further. If this approach is to be followed, we recommend that the dependency of SWE on the coefficient α is investigated and then included in the algorithm.

The grain size determines how sensitive the microwaves are to the snow. For a given frequency the microwaves will be more sensitive to larger grains than to smaller ones. For a given grain size, higher frequencies are more sensitive to snow than lower ones. One

should therefore consider using more than one frequency to separate the SWE signals from those of SGS. (Foster *et al.* 2005)

Algorithms derived from the classical spectral gradient algorithm (Chang *et al.* 1987) apply the spectral difference between 19 and 39 GHz, assuming that the lower frequency is insensible to snow. This assumption may fail for large grains sizes as well as for thick snow layers. A lower frequency, though, will be less sensitive and may therefore better serve as a reference in the spectral difference approach. Furthermore, when a sensitive higher frequency reaches or approaches the level of saturation, it will become less sensitive and will thus underestimate the snow variables. In such cases, which may be caused by large grain sizes, it should be considered to use a less sensitive, lower frequency.

Model simulations have been used for the investigation of how snow depth retrievals are affected by the evolution of the grain size and other physical properties of the snow (Markus *et al.* 2006). Their results suggest that a combination of the 10, 19, 37, and 89 GHz frequencies will improve retrieval accuracy, but a snow thickness of 30 cm is necessary to obtain a significant spectral difference between the two lowest frequencies.

Other issues

Derksen (2008) examined low frequency bands of AMSR-E and found that the general SWE performance improved by using the spectral difference $T_{V19} - T_{V10}$. This difference was less influenced by other factors than the SWE. This finding is in accordance with the difference in sensitivity for snow grain size between 39GHz and 19GHz. They also found that the new spectral difference was less sensitive to forest vegetation. A multi-frequency approach combining $T_{V19} - T_{V10}$ and $T_{V39} - T_{V19}$ appear as appropriate (Derksen 2008), but the influence of the forest cover should be considered when 39 GHz is included.

From an operational point of view, the utilization of 10 GHz is problematic. This frequency has been absent since SMMR was substituted by SSM/I, and will not be available until GCOM-W is operational. Currently there are also uncertainties concerning NPOESS microwave instrumentation.

The retrieval of snow variables from microwave data is still a field in development. Snow cover detection algorithms are quite simple and reliable. Snow volume algorithms may work well under given conditions, but may fail at others. Much of the research in the area is still focusing on models for the interaction between the snow and the microwaves emitted from it. These models are developing in complexity with respect to the vertical structure of the snow pack, but the spatial variability also needs to be considered. In the Encyclopaedia of Hydrological Sciences, Hall *et al*. (2005) states: "It is well accepted that there is no algorithm that is ideal globally."

6 Current operational and prototype products and services

6.1 NSIDC

The acronym NSIDC stands for USA's National Snow and Ice Data Center. Data produced by NSIDC are in general represented in the NSIDC Equal-Area Scalable Earth Grid (EASE-Grid). NSIDC offers these products:

Global Monthly EASE-Grid Snow Water Equivalent Climatology

This data set (http://nsidc.org/data/nsidc-0271.html) comprises global, monthly satellite-derived SWE records from November 1978 through June 2003. Global data are gridded to the Northern and Southern 25 km EASE-Grids. Global SWE data have been derived from SMMR and SSM/I. The data have been enhanced with snow cover frequencies derived from the Northern Hemisphere EASE-Grid Weekly Snow Cover and Sea Ice Extent Version 2 data. These data are suitable for studies of continental-scale time-series of snow cover and SWE.

The data are binary data files and PNG images, which are available via FTP. Data access is unrestricted, but it is recommended that users register before accessing the data. Registered users automatically receive e-mail notification of product updates and changes to the processing.

Northern Hemisphere EASE-Grid Weekly Snow Cover

The Northern Hemisphere EASE-Grid Weekly Snow Cover and Sea Ice Extent Version 3 product and Version 3.1 update (http://nsidc.org/data/nsidc-0046.html) contains snow cover data at weekly intervals from 3 October 1966 through 24 June 2007. From 23 October 1978 the product is a combined one of snow cover and sea ice extent.

The data set is the first representation of combined snow and sea ice measurements derived from satellite observations for this period. The data are designed to facilitate studies of Northern Hemisphere seasonal fluctuations of snow cover and sea ice extent, and are provided in the Northern Hemisphere 25 km EASE-Grid.

Snow cover extent is based on the digital NOAA-NESDIS Weekly Northern Hemisphere Snow Charts, revised by D. Robinson (Rutgers University) and regridded to the EASE-Grid. The original NOAA-NESDIS weekly snow charts are derived from the manual interpretation of AVHRR, GOES, and other visible-band satellite data. Sea ice extent is regridded to EASE-Grid from Sea Ice Concentrations from Nimbus-7 SMMR and DMSP SSM/I Passive Microwave Data.

AMSR-E

The AMRS-E sensor onboard EOS Aqua is processed to retrieve global EASE-grids of SWE (snow water equivalent), with a cell size of 25 km. The grids in this system are predefined. The Level 3 SWE products are aggregated from all orbits, and are available as daily, pentad (5 days) and monthly data sets. The HDF-files, 2.1 MB each, are available via ftp. NOTE

that the unit in the product is 2 mm, which means that the values in the files should be multiplied by 2.

It is requested that the use of the data distributed by NSIDC is acknowledged by a citation, see http://nsidc.org/data/docs/daac/ae_swe_ease-grids.gd.html:
"Kelly, Richard E. J., Alfred T. C. Chang, James L. Foster, and Marco Tedesco. 2004, updated daily. *AMSR-E/Aqua Daily L3 Global Snow Water Equivalent EASE-Grids* V002, [list the dates of the data used]. Boulder, Colorado USA: National Snow and Ice Data Center. Digital media."

6.2 Others

Passive microwave SWE data for the Canadian Prairies

This product is produced by as apart of the Canadian National Snow Information System for Water (NSISW) within the framework of "State of the Canadian Cryosphere" (SOCC), see www.socc.ca. Data are available from 1978 to present, and are gridded to the EASE grid (25 km). The sensors include SMMR, SSM/I, and AMSR_E. The product is a regional product for Western Canada.

Eurasian Snow Cover monitoring

The Finnish Meteorological Institute (FMI) has produced snow maps showing snow depth, and snow water equivalent since March 2007. In addition, snow melt maps are available from January 2008. The products are generated from AMRS-E and SSM/I microwave data, combined with ancillary data. The maps cover the Eurasian continent north of 50 °N and are represented by a 0.25 ° lat-lon grid.

7 Discussion and conclusions

The characteristic difference in brightness temperature between two microwave frequencies is a signature that is unique for snow covered land surfaces. The reduction in brightness temperature is most prominent at higher frequencies. A positive value of the typical spectral difference T_{19}-T_{37} is considered as a reliable indicator of dry snow cover. Alternatively, a threshold different from 0 can be used for the snow cover detection. Wet snow is much more difficult, but can be indicated by means of the difference in brightness temperature between horizontal and vertical polarizations.

The quantification of the snow cover in terms of snow water equivalent (SWE) is a more demanding task. Firstly, there is an ambiguity between SWE and snow depth (SD). Secondly, the spectral difference depends not only on the SWE, but also on other snow features, on vegetation above the snow surface, and on the ground beneath the snow pack.

Since the snow volume can be quantified in terms of SWE or in terms of SD, there may be an ambiguity in the algorithms. When algorithms are developed, they have to be calibrated against ground observations, and they are typically expressed in terms of linear regression functions (e.g. Chang *et al.* 1987). Global algorithms require a global net of observations, which are available from weather stations. These data include measurements of SD, while SWE measurements are more rare. The calibration of SWE algorithms has therefore assumed some snow density, usually 0.3 kg/dm^3, in order to convert SD observations to SWE values. From a physical point of view the microwave signature depends on SWE, and not on SD, so the algorithms should therefore be considered as SWE algorithms even though they happen to be expressed in terms of SD. However, since their calibration is based on SD data, assuming some snow density, the algorithm may have a tendency to become biased when the density differs from the assumed one.

Empirical algorithms developed for limited areas may work well as long as the conditions do not differ too much from the conditions assumed in the development of the algorithm. For larger regions, simple empirical algorithms will reveal too large uncertainties during calibration because of the unconsidered factors. The effects of these features can be addressed in different ways.

One approach is to develop different algorithms for different areas, or rather for different nature types, and then apply the most appropriate algorithm for each microwave observation (Tait 1998), i.e. a hierarchical approach. This will typically yield different estimates depending on which formula that is chosen for the given microwave observation. This may be a problem when the ground class is unknown, uncertain, or mixed. The mixture of ground classes within the large resolution cells has motivated the Canadian development of algorithms that combine estimates for various ground classes into an aggregated estimate (Derksen *et al.* 2005a). However, when moving from a national to a global scale, the classification scheme must be developed further, or at least validated thoroughly, in order to make this approach reliable.

Another approach is to consider these factors directly, either by estimating them from other sources or to develop algorithms that estimate these variables together with the SWE. These algorithms may be based on radiative transfer models that consider these variables

simultaneously. In practice, some factors often need to be ignored or set to some assumed values, while addressing other ones.

The influence from the ground beneath the snow seems to have been ignored in many algorithms, but have been addressed by the HUT research group. In an early stage they considered the change in the spectral difference from pre-snow conditions to that of the situation under consideration (Hallikainen and Jolma 1986), instead of the spectral difference itself. Later they have included the radiation from the ground in their radiative transfer model (Pulliainen *et al.* 1999). Other approaches assume that these effects are cancelled out by the spectral difference calculation.

The reduction of the characteristic snow signature created by forest cover and other types of vegetation above the snow, causes a situation that can be handled in several ways. Hierarchical approaches will typically include vegetation cover as one of their components. The Canadian algorithm considers a mixture of 4 forest classes (Derksen *et al.* 2005b). Another approach is to include the vegetation in radiative transfer models, which has been done in the HUT model.

The snow grain size (SGS) is likely the most important variable in addition to the SWE. Both variables will contribute positively to the spectral difference. It is difficult to separate the two factors from each other.

Under some special conditions, the snow metamorphosis will cause SWE and SGS to be negatively correlated to each other, which will corrupt simple algorithms completely. An algorithm trying to solve this dilemma by considering the temporal development of the temperature gradient (Josberger and Mognard 2002) have showed good results in very cold regions. Although this approach have been refined and developed further (Grippa *et al.* 2004; Biancamaria *et al.* 2008), no convincing way of delimiting the domain for the use of this algorithm has yet been demonstrated.

The scattering caused by the snow depends on the ratio between grain size and the microwave wavelength, which suggests that the grain size can be determined by using more than one spectral difference. However, operational applications are limited by the channels available on operational missions, like the SSM/I.

In general, the combined effect of SWE and grain size is modelled in most radiative transfer models. Inversion of current radiative models is not able to separate the various properties from each other with sufficient certainty. Some assumptions concerning some of the snow characteristics have to be made in order to invert the radiative models. These assumptions may be based on observations or on geophysical models that takes the spatial distribution and/or temporal development into account.

The HUT model considers both the grain size and the SWE. Pulliainen's (2006) algorithm is based on the HUT model (Pulliainen *et al.* 1999), and it includes observations from globally distributed weather stations in order to estimate and interpolate the grain size parameter in the model. This algorithm differs from other algorithms in a few important points. It considers both the temporal and the spatial structure of the variables. The estimations need to be in accordance with their preceding values and with the expected development pattern. Furthermore, the algorithm uses the grain size as the fitting parameter for the model esti-

mations instead of considering some arbitrary regression coefficient. Validations for Eurasia yielded an RMS error for SD estimations of approximately 15 cm (Pulliainen 2006).

It should be noted that the HUT model does not consider the influence of the internal layering in the snow pack, which is important. Internal layers will increase scattering in the snow pack, and thereby change the spectral gradient. The Swiss MEMLS model (Mätzler and Wiesmann 1999) considers the internal layering in the snow pack, but ignores the vegetation structure. Besides, the MEMLS model is too complex to be used directly in algorithms (Mätzler 2006).

It is therefore suggested that a microwave algorithm for global snow cover estimation should be funded on Pulliainen's (2006) algorithm. An alternative could possible be a modification of the NSIDC algorithm (Chang and Rango 2000). In any case, data from global weather stations as well as global land cover maps will be crucial.

It should be noted that one single algorithm that yields good estimates for SWE globally does not exist. Unsolved issues include optimal choice of microwave channels, combination of optical and microwave radiometry, complex mountainous terrain, integration of RT models with geophysical models for snow metamorphosis, etc.

References

Armstrong, R L and M J Brodzik (2001). "Recent Northern Hemisphere snow extent: A comparison of data derived from visible and microwave satellite sensors." *Geophysical Research Letters* **28**(19): 3673-3676.

Armstrong, R L and M J Brodzik (2002). Hemispheric-scale comparison and evaluation of passive-microwave snow algorithms. *Annals of Glaciology, Vol 34, 2002*. Cambridge, Int Glaciological Soc. **34:** 38-44.

Aschbacher, J (1989). Land surface studies and atmosheric effects by satellite microwave radiometry, University of Insbruck. **PhD**.

Bernier, P Y (1987). "Microwave remote-sensing of snowpack properties - Potential and limitations." *Nordic Hydrology* **18**(1): 1-20.

Biancamaria, S, N M Mognard, A Boone, M Grippa and E G Josberger (2008). "A satellite snow depth multi-year average derived from SSM/I for the high latitude regions." *Remote Sensing of Environment* **112**(5): 2557-2568.

Boone, A, N Mognard, B Decharme, H Douville, M Grippa and K Kerrigan (2006). "The impact of simulated soil temperatures on the estimation of snow depth over Siberia from SSM/I compared to a multi-model climatology." *Remote Sensing of Environment* **101**(4): 482-494.

Brown, R, C Derksen and L Wang (2007). "Assessment of spring snow cover duration variability over northern Canada from satellite datasets." *Remote Sensing of Environment* **111**(2-3): 367-381.

Chang, A T C (1986). *Nimbus-7 SMMR snow cover data*. Snow Watch'85 Proceeedings of the workshop, University of Maryland, College Park, MD, World Data Center A for Glaciology (Snow and Ice), Boulder, Colorado.

Chang, A T C, J L Foster and D K Hall (1987). "Nimbus-7 SMMR derived global snow cover parameters." *Annals of Glaciology* **9**: 39-44.

Chang, A T C, J L Foster and D K Hall (1996). "Effects of forest on the snow parameters derived from microwave measurements during the Boreas Winter Field Campaign." *Hydrological Processes* **10**(12): 1565-1574.

Chang, A T C, J L Foster, D K Hall, B E Goodison, A E Walker, J R Metcalfe and A Harby (1997). "Snow parameters derived from microwave measurements during the BOREAS winter field campaign." *Journal of Geophysical Research-Atmospheres* **102**(D24): 29663-29671.

Chang, A T C and A Rango (2000). Algorithm theoretical basis document (ATBD) for the AMSR-E snow water equivalent algorithm, NASA.

Derksen, C, A Walker, E LeDrew and B Goodison (2002). Time-series analysis of passive-microwave-derived central North American snow water equivalent imagery. *Annals of Glaciology, Vol 34, 2002*. **34:** 1-7.

Derksen, C, A Walker and B Goodison (2005a). "Evaluation of passive microwave snow water equivalent retrievals across the boreal forest/tundra transition of western Canada." *Remote Sensing of Environment* **96**(3-4): 315-327.

Derksen, C, A E Walker, B E Goodison and J W Strapp (2005b). "Integrating in situ and multiscale passive microwave data for estimation of subgrid scale snow water equivalent distribution and variability." *IEEE Transactions on Geoscience and Remote Sensing* **43**(5): 960-972.

Derksen, C (2008). "The contribution of AMSR-E 18.7 and 10.7 GHz measurements to improved boreal forest snow water equivalent retrievals." *Remote Sensing of Environment* **112**(5): 2701-2710.

Foster, J L, A T C Chang and D K Hall (1997). "Comparison of snow mass estimates from prototype passive microwave snow algorithm, a revised algorithm and a snow depth climatology." *Remote Sensing of Environment* **62**(2): 132-142.

Foster, J L, C J Sun, J P Walker, R Kelly, A Chang, J R Dong and H Powell (2005). "Quantifying the uncertainty in passive microwave snow water equivalent observations." *Remote Sensing of Environment* **94**(2): 187-203.

Goïta, K, A E Walker and B E Goodison (2003). "Algorithm development for the estimation of snow water equivalent in the boreal forest using passive microwave data." *International Journal of Remote Sensing* **24**(5): 1097-1102.

Goodison, B E (1989). *Determination of areal snow water equivalent on the Canadian prairies using passive microwave satellite data*. International Geoscience and Remote Sensing Symposium, Vancouver, Canada, IEEE.

Goodison, B E, A E Walker and F W Thirkettle (1990). Determination of snow water equivalent on the Canadian Prairies using near real-time passive microwave data. *Workshop Applications of Remote Sensing in Hydrology*. Saskatoon, Canada, Environment Canada**:** 297-309.

Grippa, M, N Mognard, T Le Toan and E G Josberger (2004). "Siberia snow depth climato logy derived from SSM/I data using a combined dynamic and static algorithm." *Remote Sensing of Environment* **93**(1-2): 30-41.

Grody, N C and A N Basist (1996). "Global identification of snowcover using SSM/I measurements." *IEEE Transactions on Geoscience and Remote Sensing* **34**(1): 237-249.

Hall, D K (1986). *Influence of snow structure variability on global snow depth measurement using microwave radiometry*. Snow Watch'85 Proceeedings of the workshop, University of Maryland, College Park, MD, World Data Center A for Glaciology (Snow and Ice), Boulder, Colorado.

Hall, D K, R E J Kelly, J L Foster and A T C Chang (2005). Estimation of Snow Extent and Snow Properties. *Encyclopedia of Hydrological Sciences***:** 811-829.

Hallikainen, M T (1984). "Retrieval of Snow Water Equivalent from Nimbus-7 Smmr Data - Effect of Land-Cover Categories and Weather Conditions." *IEEE Journal of Oceanic Engineering* **9**(5): 372-376.

Hallikainen, M T and P A Jolma (1986). "Retrieval of the Water Equivalent of Snow Cover in Finland by Satellite Microwave Radiometry." *IEEE Transactions on Geoscience and Remote Sensing* **24**(6): 855-862.

Hallikainen, M T and P A Jolma (1992). "Comparison of Algorithms for Retrieval of Snow Water Equivalent from Nimbus-7 Smmr Data in Finland." *IEEE Transactions on Geoscience and Remote Sensing* **30**(1): 124-131.

Halllikanen, M (1989). "Microwave radiometry of snow." *Advances in Space Research* **9**(1): 267-275.

Hiltbrunner, D (1996). Land surface temperature and microwave emissivity from SSM/I data. *Institute of Applied Physics*. Bern, University of Bern. **PhD**.

Hofer, R and E Schanda (1978). "Signatures of snow in 5 to 94 GHz range." *Radio Science* **13**(2): 365-369.

Hollinger, J P, R Lo, G A Poe, R C Savage and J L Peirce (1987). Special Sensor Microwave/Imager User's Guide. Washington, D.C., Naval Research Laboratory.

Jiang, L M, J C Shi, S B Tjuatja, J Dozier, K S Chen and L X Zhang (2007). "A parameterized multiple-scattering model for microwave emission from dry snow." *Remote Sensing of Environment* **111**(2-3): 357-366.

Josberger, E G and N M Mognard (1998). *Northern Great Plains snowpack hydrology from satellite passive microwave observations*, IEEE.

Josberger, E G and N M Mognard (2002). "A passive microwave snow depth algorithm with a proxy for snow metamorphism." *Hydrological Processes* **16**(8): 1557-1568.

Kelly, R and A Chang (2003). "Development of a passive microwave global snow depth retrieval algorithm for Special Sensor Microwave Imager (SSM/I) and Advance Microwave Scanning Radiometer-EOS (AMSR-E) data." *Radio Science* **38**(4): 8076.

Kelly, R E, A T Chang, L Tsang and J L Foster (2003). "A prototype AMSR-E global snow area and snow depth algorithm." *IEEE Transactions on Geoscience and Remote Sensing* **41**(2): 230-242.

Kelly, R E J and J L Foster (2005). The AMSR-E snow water equivalent product: Status and future development. *Poster presented at American Geophysical Union fall meeting*. San Francisco.

Kelly, R E J, J L Foster and D K Hall (2005). The AMSR-E snow water equivalent product: Algorithm development and progress in product validation. *Poster presented at the Proceedings of the 28th General Assembly of the Union of International Radio Science*. New Dehli, India.

Künzi, K F, S Patil and H Rott (1982). "Snow-cover parameters retrieved from Nimbus-7 Scanning Multichannel Microwave Radiometer (SMMR) data." *IEEE Transactions on Geoscience and Remote Sensing* **20**(4): 452-467.

Kärnä, J P, J Lemmetyinen, M Hallikainen, P Lahtinen, J Pulliainen and M Takala (2007). *Operational snow map production for whole Eurasia using microwave radiometer and ground-based observations*. IEEE International Geoscience and Remote Sensing Symposium (IGARSS), Barcelona, SPAIN.

Macelloni, G, S Paloscia, P Pampaloni and M Tedesco (2001). "Microwave emission from dry snow: A comparison of experimental and model results." *IEEE Transactions on Geoscience and Remote Sensing* **39**(12): 2649-2656.

Markus, T, D C Powell and J R Wang (2006). "Sensitivity of passive microwave snow depth retrievals to weather effects and snow evolution." *IEEE Transactions on Geoscience and Remote Sensing* **44**(1): 68-77.

McFarland, M J, G D Wilke and P H Harder (1987). "Nimbus-7 SMMR investigation of snowpack properties in the northern great-plains for the winter of 1978-1979." *IEEE Transactions on Geoscience and Remote Sensing* **25**(1): 35-46.

Mognard, N M, E G Josberger and P Gloersen (1998). *Seasonal evolution of the 1988-89 Northern Great Plains snowpack from satellite passive microwave observations*. 27th International Symposium on Remote Sensing of Environment, Tromso, Norway.

Mätzler, C, E Schanda and W Good (1982). "Towards the definition of optimum sensor specifications for microwave remote-sensing of snow." *IEEE Transactions on Geoscience and Remote Sensing* **20**(1): 57-66.

Mätzler, C (1987). "Applications of the interaction of microwaves with the natural snow cover." *Remote sensing reviews* **2**: 259-387.

Mätzler, C and R Hüppi (1989). "Review of signature studies for microwave remote sensing of snowpacks." *Advances in Space Research* **9**(1): 253-265.

Mätzler, C (1994). "Passive microwave signatures of landscapes in winter." *Meteorology and Atmospheric Physics* **54**(1-4): 241-260.

Mätzler, C and A Wiesmann (1999). "Extension of the microwave emission model of layered snowpacks to coarse-grained snow." *Remote Sensing of Environment* **70**(3): 317-325.

Mätzler, C, Ed. (2006). *Thermal microwace radiation: applications for remote sensing*. IET electromagnetic waves series London, The Institution of Engeneering and Technology.

Mätzler, C, A Wiesman, J Pulliainen and M Hallikainen (2006). Microwave emission of snow. *Thermal microwace radiation: applications for remote sensing*. C Mätzler. London, The Institution of Engeneering and Technology**:** 371- 382.

Nagler, T (1991). Verfahren zur Analyse de Schneebedeckung aus Messungen des SSM/I *University of Innsbruck*. **Diplomarbeit**.

Pardé, M, K Goita and A Royer (2007). "Inversion of a passive microwave snow emission model for water equivalent estimation using airborne and satellite data." *Remote Sensing of Environment* **111**(2-3): 346-356.

Pulliainen, J and M Hallikainen (2001). "Retrieval of regional snow water equivalent from space-borne passive microwave observations." *Remote Sensing of Environment* **75**(1): 76-85.

Pulliainen, J (2006). "Mapping of snow water equivalent and snow depth in boreal and sub-arctic zones by assimilating space-borne microwave radiometer data and ground-based observations." *Remote Sensing of Environment* **101**(2): 257-269.

Pulliainen, J T, J Grandell and M T Hallikainen (1999). "HUT snow emission model and its applicability to snow water equivalent retrieval." *IEEE Transactions on Geoscience and Remote Sensing* **37**(3): 1378-1390.

Singh, P R and T Y Gan (2000). "Retrieval of snow water equivalent using passive microwave brightness temperature data." *Remote Sensing of Environment* **74**(2): 275-286.

Solberg, R, D Hiltbrunner, J Koskinen, T Guneriussen, K Rautiainen and M Hallikainen (1997). Snow algorithms and products. Review and recommendations for research and development. *NR report*. Oslo, Norsk Regnesentral**:** 111.

Stiles, W H and F T Ulaby (1980). "The active and passive microwave response to snow parameters .1. Wetness." *Journal of Geophysical Research-Oceans and Atmospheres* **85**(NC2): 1037-1044.

Sturm, M, J Holmgren and G E Liston (1995). "A Seasonal Snow Cover Classification-System for Local to Global Applications." *Journal of Climate* **8**(5): 1261-1283.

Tait, A and R Armstrong (1996). "Evaluation of SMMR satellite-derived snow depth using ground-based measurements." *International Journal of Remote Sensing* **17**(4): 657-665.

Tait, A, D Hall, J Foster, A Chang and A Klein (1999). "Detection of snow cover using millimeter-wave imaging radiometer (MIR) data." *Remote Sensing of Environment* **68**(1): 53-60.

Tait, A B (1998). "Estimation of snow water equivalent using passive microwave radiation data." *Remote Sensing of Environment* **64**(3): 286-291.

Tait, A B, D K Hall, J L Foster and R L Armstrong (2000). "Utilizing multiple datasets for snow-cover mapping." *Remote Sensing of Environment* **72**(1): 111-126.

Tait, A B, J S Barton and D K Hall (2001). "A prototype MODIS-SSM/I snow-mapping algorithm." *International Journal of Remote Sensing* **22**(17): 3275-3284.

Tedesco, M and E J Kim (2006). "Intercomparison of electromagnetic models for passive microwave remote sensing of snow." *IEEE Transactions on Geoscience and Remote Sensing* **44**(10): 2654-2666.

Tedesco, M, E J Kim, A W England, R D De Roo and J P Hardy (2006). "Brightness temperatures of snow melting/refreezing cycles: Observations and modeling using a multilayer dense medium theory-based model." *IEEE Transactions on Geoscience and Remote Sensing* **44**(12): 3563-3573.

Tedesco, M and J Miller (2007). "Observations and statistical analysis of combined active-passive microwave space-borne data and snow depth at large spatial scales." *Remote Sensing of Environment* **111**(2-3): 382-397.

Tiuri, M E (1982). "Theoretical and experimental studies of microwave emission signatures of snow." *IEEE Transactions on Geoscience and Remote Sensing* **20**(1): 51-57.

Ulaby, F T and W H Stiles (1980). "The active and passive microwave response to snow parameters .2. Water equivalent of dry snow." *Journal of Geophysical Research-Oceans and Atmospheres* **85**(NC2): 1045-1049.

Walker, A E and B E Goodison (1992). *Discrimination of a wet snow cover using passive microwave satellite data*. 1992 International Symposium on Remote Sensing of Snow and Ice, Boulder, Co.

Walker, A E and B E Goodison (1993). "Discrimation of a wet snow cover using passive microwave data." *Annals of Glaciology* **17**: 307-311.

Wiesmann, A, C Matzler and T Weise (1998). "Radiometric and structural measurements of snow samples." *Radio Science* **33**(2): 273-289.

Wiesmann, A and C Mätzler (1999). "Microwave emission model of layered snowpacks." *Remote Sensing of Environment* **70**(3): 307-316.

Woodhouse, I H (2006). *Introduction to microwave remote sensing*, Tayor & Francis.